Energy, Mines and Resources Canada

Énergie, Mines et Ressources Canada

CANMET

Canada Centre for Mineral and Energy Technology

Centre canadien de la technologie des minéraux et de l'énergie

Mining Research Laboratories

Laboratoires de recherche minière

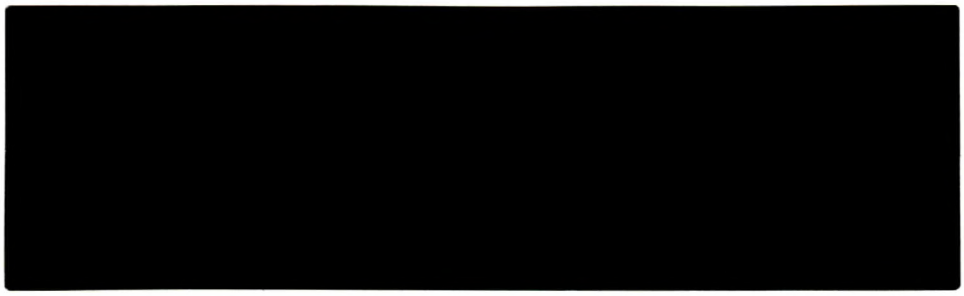

Canada

MIGRATION OF ACIDIC GROUNDWATER SEEPAGE FROM URANIUM-TAILINGS IMPOUNDMENTS, 1. FIELD STUDY AND CONCEPTUAL HYDROGEOCHEMICAL MODEL

Kevin A. Morin, John A. Cherry, Nand K. Dave,
TJoe P. Lim and AL J. Vivyurka

MRL 88-130 (J)

Published in Journal of Contaminant Hydrology, Volume 2,
Pp. 271-303, 1988.

Journal of Contaminant Hydrology, 2 (1988) 271–303
Elsevier Science Publishers B.V., Amsterdam — Printed in The Netherlands

MIGRATION OF ACIDIC GROUNDWATER SEEPAGE FROM URANIUM-TAILINGS IMPOUNDMENTS, 1. FIELD STUDY AND CONCEPTUAL HYDROGEOCHEMICAL MODEL

KEVIN A. MORIN,[1,*], JOHN A. CHERRY[2], NAND K. DAVÉ[3], TJOE P. LIM[3] and AL J. VIVYURKA[4]

[1]*Morwijk Enterprises, Suite 1706L, 1600 Beach Ave., Vancouver, B.C. V6G 1Y6, Canada*
[2]*Institute for Groundwater Research, University of Waterloo, Waterloo, Ont. N2L 3G1, Canada*
[3]*Elliot Lake Laboratories, CANMET, Energy, Mines, and Resources Canada, P.O. Box 100, Elliot Lake, Ont. P5A 2J6, Canada*
[4]*Rio Algom Limited, P.O. Box 1500, Elliot Lake, Ont. P5A 2K1, Canada.*

(Received November 19, 1986; revised and accepted December 11, 1987)

ABSTRACT

Morin, K.A., Cherry, J.A., Davé, N.K., Lim, T.P. and Vivyurka, A.J., 1988. Migration of acidic groundwater seepage from uranium-tailings impoundments, 1. Field study and conceptual hydrogeochemical model. *J. Contam. Hydrol.*, 2: 271–303.

In this first paper of a series, the results of a study at a non-operational tailings site are presented and are used to construct a general conceptual model for seepage migration from uranium-tailings impoundments. Many parts of the model are applicable to other types of tailings and to acid drainage in general.

At the field site, the impoundment lies over a portion of a glaciofluvial sand aquifer. Tailings seepage drains downward into the aquifer and then migrates laterally away. Results of the field study indicate the seepage can be divided into three geochemical zones: (1) the inner core, which is essentially unaltered, acidic seepage from the tailings; (2) the neutralization zone, in which inner-core water is neutralized and aqueous concentrations decrease significantly; and (3) the outer zone, which contains both neutralized water from the neutralization zone and pH-neutral process water from the uranium milling operation. Yearly comparisons from 1979 to 1984 indicate the neutralization zone and inner core are migrating downgradient at a rate of about 1 meter/year, which is about 1/440 of the groundwater velocity. The mechanisms that produce the retardation and the decreases in aqueous concentrations are part of the conceptual model.

The main features of the conceptual model are solid-liquid interactions, particularly mineral precipitation-dissolution, and buffering effects of dominant aqueous species. The important minerals undergoing precipitation-dissolution are the calcite-siderite solid solution, gypsum, Al-OH minerals, and Fe-OH minerals. "Cell and streamtube" calculations are used to evaluate the general trends in aqueous concentrations and to assist in explaining observed migration rates. Co-precipitation with the above minerals apparently accounts for decreases in other major, minor, and metal solutes. Because of the large amount of mineral precipitation and co-precipitation, variations in ^{2}H and ^{18}O were observed over a flow distance of several meters, while ^{13}C remained essentially constant.

0169-7722/88/$03.50

1. INTRODUCTION

Within the last decade, the interest in environmental interactions between surface-impounded mine-mill tailings and their surrounding environments has grown rapidly. This interest in uranium tailings is particularly intense because of the toxicity of several radionuclides at extremely low concentrations ($< 1\,ng\,L^{-1}$). The delineation of the environmental interactions requires a thorough definition of the source term, the tailings impoundment in this case, and of the pathways of interaction. In order to examine the aqueous pathway from uranium tailings, the Institute for Groundwater Research at the University of Waterloo initiated in 1978 a field study in the Elliot Lake uranium district of Ontario (Fig. 1).

The field study concentrated on the Nordic Main tailings impoundment (Fig. 2). The Nordic Main area is located in a valley between two bedrock outcrops with a glaciofluvial sand aquifer lying in the valley (Fig. 3). The impoundment was created by the construction of coarse-rock dams, which incorporate bedrock outcrops in a few locations. (Fig. 2), followed by the filling of the area between the dams and the north valley wall with tailings from 1957 to 1968. The tailings, which contain up to 7 weight-percent (wt.%) pyrite, were drained of

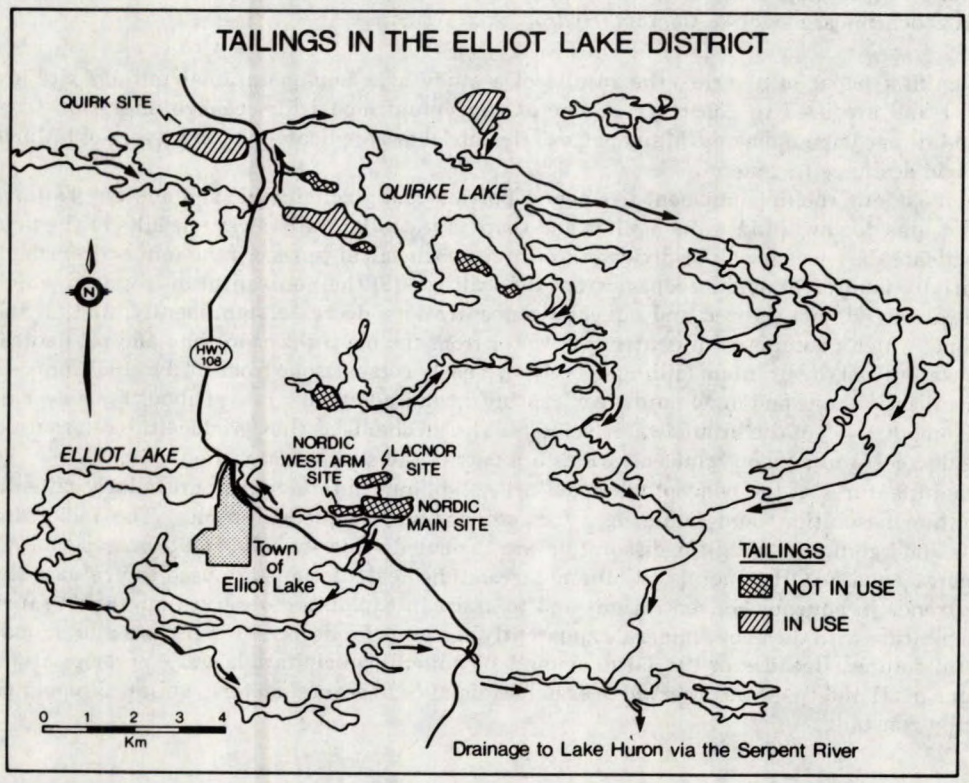

Fig. 1. Elliot Lake and surrounding area.

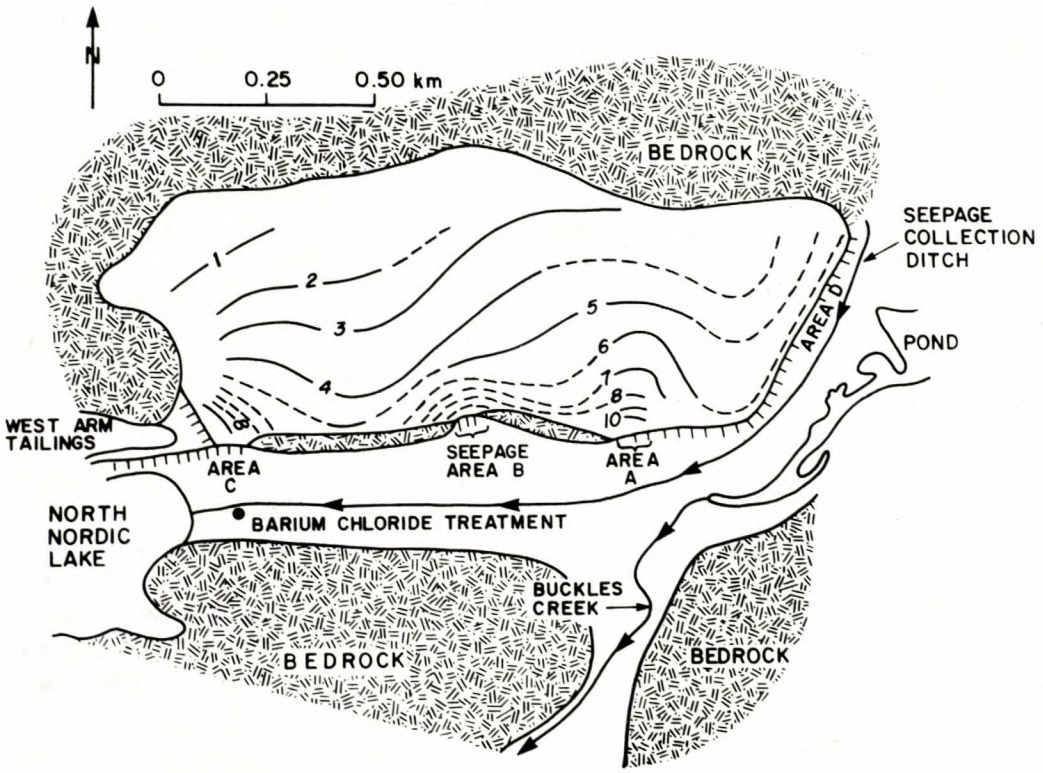

Fig. 2. Nordic Main impoundment near Elliot Lake, Ontario. Depth-to-water-table contours in the tailings from Cherry et al., 1980. (contour values in meters.)

ponded water in the late 1960's and the tailings surface was artificially vegetated through the 1970's.

The initial hydrogeologic survey of the Nordic Main area was presented in Blair et al. (1980) and Blair (1981). Following the initial survey, the field study was divided into several specific topics: groundwater–surface-water interactions on the tailings (Blowes, 1983; Abdul and Gillham, 1984), the aqueous and gaseous phases of the tailings unsaturated zone (Smyth, 1981), the tailings

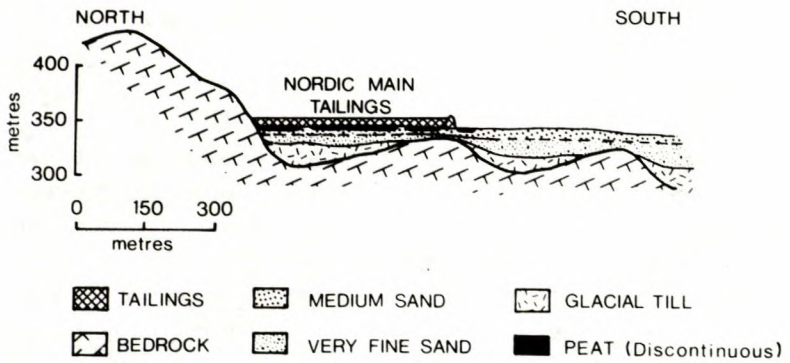

Fig. 3. Generalized north-south cross-section through the Nordic Main area.

saturated zone (Cherry et al., 1980; Dubrovsky et al., 1984, 1985; Dubrovsky, 1986), and pyrite oxidation (Nicholson, 1984). These studies provide a detailed definition of the aqueous source term, the tailings mass.

Surface-water flow at the field site occurs in a seepage-collection ditch and in Buckles Creek (Fig. 2). The ditch, which originates on the tailings surface, carries little to no water through the year in its upper reaches and collects only a minor portion of subsurface seepage in its lower reaches. Buckles Creek has no direct surface-water connection with the tailings, but receives tailings seepage through the groundwater flow system (Dubrovsky et al., 1984). Because the amount of surface water in the area is minor and because the tailings lie over a medium-grain sand bed capable of transmitting large amounts of seepage, the groundwater component of the aqueous pathway was studied in detail.

The initial description of the physical and chemical hydrogeology of the sand aquifer and the preliminary evaluation of the geochemical behavior of tailings seepage in the aquifer were presented in Morin et al. (1982) and Cherry et al. (1982). Further data collection and evaluation, as well as computer simulations of the field site and of other case studies, were given in Morin (1983). Then additional computer simulations (Cherry et al., 1984) and additional data collection and evaluation for 1983 and 1984 (Morin, 1985) were made. The purpose of this series of papers is to reassess and to integrate all of these previous studies into one presentation on the migration of groundwater seepage from uranium-tailings impoundments. This first paper presents the results of the 1979–1984 field study and develops a conceptual model for understanding and simulating the migration.

There are four sites around the perimeter of the Nordic Main impoundment through which subsurface seepage passes (Fig. 2). Seepage Area A contains the best developed acidic seepage plume and consequently this area was emphasized in the field study. Only field results from Area A are presented in this paper.

2. METHODOLOGY

This section briefly describes the methodology used for data collection in the field study. A detailed description of methodology and the rationale for the choice of methods can be found in Morin and Cherry (1987).

Piezometers installed in the glaciofluvial sand aquifer (prefix "M" on Fig. 4) are multi-level bundle-type piezometers made from polyethylene tubing. (Cherry et al., 1983). The pH and Eh of the groundwater in each piezometer were measured by continuously pumping water via a peristaltic pump through a 100-mL air-tight flow-through cell containing a combination pH electrode calibrated in nominal pH 7 and pH 4 buffers and a combination Eh electrode standardized against Zobell's redox buffer (e.g., Morin, 1986). Electrical conductance was measured with a conductance meter and probe following determination of the cell constant with KCl standards and was converted to 25°C-equivalent values. Alkalinities were measured in-field by titration with standardized

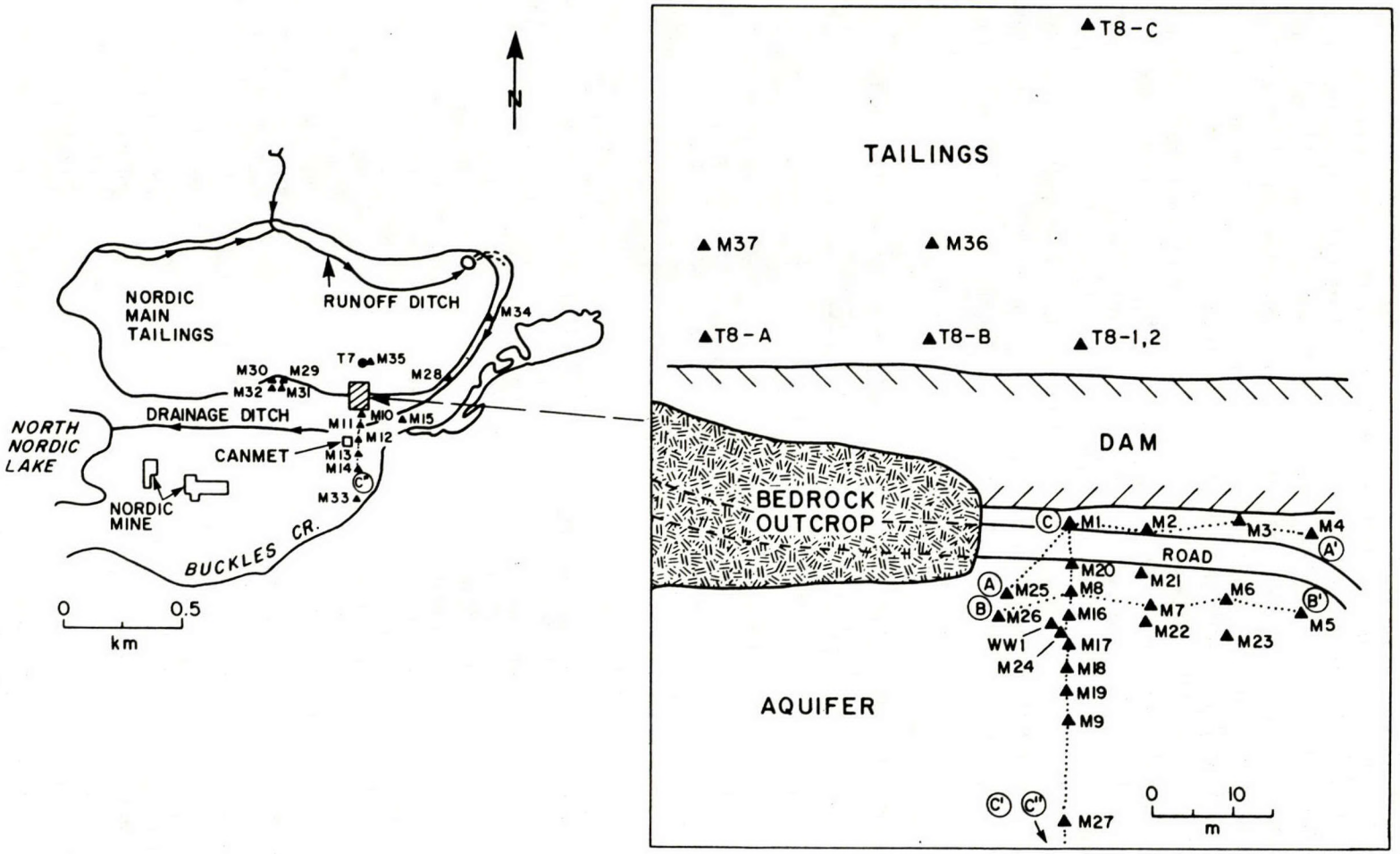

Fig. 4. Locations of piezometers in the Nordic Main area.

HCl immediately after sample collection. Water samples were filtered through 0.45 μm filters, directed into polyethylene bottles, acidified with concentrated HCl to about pH 1.5 (often requiring 30 mL acid for 1 liter of sample), and sent to laboratories for analysis of the constituents listed in Table 1. Many concentrations were reported on a mass/mass basis (ppm), but can be taken as identical on a mass/volume basis (mg L^{-1}) with minimal error. Water samples were normally collected only during summer months.

The results of water analyses and field measurements were entered as input into the chemical speciation program, WATEQ2 (Ball et al., 1979). WATEQ2 output provided concentrations and activities of free ions, ion pairs, and complexes, and provided saturation indices for many minerals.

The electroneutrality equation was used to evaluate the overall accuracy of water analyses. Mean errors were + 7.98%, + 1.10%, and + 6.18% in 1980, 1982 and 1984, respectively, where the error represents the difference between total

TABLE 1

Parameters and concentration ranges measured in Seepage Area A (concentration in ppm unless noted)

Parameter	Concentrations	Parameter	Concentrations
Field pH	3.20–6.81 pH units	Cl	170–5.5
Lab. pH	2.4–6.9 pH units	F	33–< 0.1
Field Eh	+ 114–+ 444 mV	NO_3	18–< 0.4
Field temp.	10.5 ± 1.5°C	NH_3	55.9–0.33 (as N)
		PO_4	< 0.04
Field conc.	11500–380 μS cm^{-1}	V	< 1
Fe	5930–8	Se	< 1
Ca	860–40	DOC (dissolved organic carbon)	8.0–22
Mg	702–12		
Na	152–1.2	Ra–223	83–6 pCi L^{-L}
Mn	56–0.91	Ra–226	213–1 pCi L^{-L}
Al	206–< 0.02	Pb–210	110–0.1 pCi L^{-1}
Cu	0.44–< 0.001	Th–227	600–6 pCi L^{-1}
Co	5.9–0.01	Th–228	9.7–< 0.5 pCi L^{-1}
Zn	0.50–0.004	Th-230	48–< 0.5 pCi L^{-1}
Pb	0.9–< 0.003	Th-232	11–< 0.5 pCi L^{-1}
Ni	6.0–0.015	Total Th	96–11 μg L^{-1}
Cr	0.14–< 0.01	Ac-227	319–16 pCi L^{-1}
Cd	< 0.05	U-234	204.5–14.9 pCi L^{-1}
		U-238	166.5–3.8 pCi L^{-1}
As	0.011–< 0.001	U-234/U-238	1.2–3.4
SO_4	14420–111	Total U	8500–0.4 μg L^{-1}
Field alk.	290–1 (as HCO_3)		
DIC (dissolved inorganic carbon)	86.4–21.6 (as C)	O-18	− 11.9 to − 10.2‰ SMOW
SiO_2	77.0–< 1	H-2	− 84 to − 69‰ SMOW
		C-13	− 20.8 to − 19.2‰ PDB

cations and total anions in equivalents per liter divided by one-half of the sum of total cations and anions. Because there are technical difficulties with analysis of Area A waters (Morin and Cherry, 1988a), an expanded program to examine accuracy and precision was carried out in 1984 (Morin, 1985) involving sets of replicates distributed to three laboratories. The resulting coefficients of variation (standard deviation/mean) for each laboratory for major ions and metals were variable but generally less than 0.037. Much higher coefficients were obtained for species with concentrations less than 1 ppm.

Solid samples of aquifer material for chemical analysis were taken from auger flights during exploratory drilling and piezometer installation. Also, a 1-m continuous core was obtained by driving an air-tight 5-cm-diameter aluminum tube into the aquifer.

3. HYDROSTRATIGRAPHY OF THE NORDIC MAIN AREA AND PHYSICAL HYDROGEOLOGY OF SEEPAGE AREA A

The shallow hydrostratigraphy of the Nordic Main area consists of several distinct units (Fig. 3). The deepest layer examined in this study is metasedimentary bedrock, which crops out to form the north and south valley walls and crops out in a few locations within the valley. This rock is fractured and has a general bulk hydraulic conductivity of $10^{-8}\,m\,s^{-1}$ in the Elliot Lake area. This basal layer is considered relatively impermeable although chemical data suggest a portion of tailings seepage may enter the fracture network and eventually discharge downgradient into the overlying sand aquifer. Deposits of till apparently lie in depressions of the bedrock surface. Neither bedrock nor till could be penetrated with augers at the site.

The glaciofluvial sand aquifer covers the bedrock and till, and is composed of two layers. The lower sand is a light gray, very-fine-grain (d_{50} = 0.12 mm) sand, varies in thickness generally from 3 to greater than 8 m, and has a specific gravity of 2.87 and a porosity of 35%. The hydraulic conductivity of the lower sand is about $5 \times 10^{-5}\,m\,s^{-1}$, based on calculations from grain-size analyses using the method of Masch and Denny (1966). A thin silt layer locally separates the lower and upper sand.

Most of the acidic seepage in Area A passes through the upper sand and, thus, the examination of this layer was emphasized. The upper sand is a dark tan, well-sorted, medium-grain (d_{50} = 0.45 mm) sand, varies in thickness from approximately 4 to 8 m, and has a porosity of 36%. The upper sand has a relatively high specific gravity of 2.98 because of a significant amount of magnetite and other heavy minerals.

The hydraulic conductivity of the upper sand was measured in several ways. A pump test near the Nordic West Arm tailings yielded a value of 1.4 to $2.2 \times 10^{-4}\,m\,s^{-1}$ and recovery data indicated $1.2 \times 10^{-4}\,m\,s^{-1}$. Permeameter tests on disturbed samples resulted in a value of $2.1 \times 10^{-4}\,m\,s^{-1}$. Calculations from four grain-size analyses using the method of Masch and Denny (1966) gave an average of $1.2 \times 10^{-4}\,m\,s^{-1}$. A borehole dilution test yielded a value of $1.0 \times 10^{-4}\,m\,s^{-1}$ from a calculation using Darcy's Law and measured values of

porosity and hydraulic gradient. Vertical-plane finite-element modelling of Area A yielded a satisfactory match to observed heads by using a conductivity of $1.2 \times 10^{-4} m s^{-1}$ and a horizontal-vertical anisotropy of 10:1, which is reasonable for a glaciofluvial sand. Changing the conductivity by a factor of 2 or anisotropy by a factor of 10 during modelling produced poorer matches.

The next hydrostratigraphic unit is peat, which lies under most of the tailings except near the dam. This peat layer is discontinuous through much of Area A.

The upper sand and peat, where present, are overlain within the impoundment boundaries by up to 10 m of tailings and within Area A by up to 1.5 m of artificially placed cobble-sand. The cobble-sand is unsaturated, but apparently would allow rapid infiltration of precipitation. Finite-element simulations indicate that infiltration to the water table in Area A up to an amount equal to yearly precipitation has an insignificant effect on groundwater flow rates and directions, because of the large groundwater velocity and volume passing through the area. As a result, the flow rates and directions of seepage leaving the tailings impoundment determine the flow characteristics in Area A.

Because relatively impermeable peat lies under much of the tailings impoundment and because the tailings mass has strong horizontal stratification (Dubrovsky, 1986), groundwater movement within the impoundment is predominately lateral towards the coarse-rock dam, where peat is absent, with subsequent downward drainage into the upper sand and then continued lateral

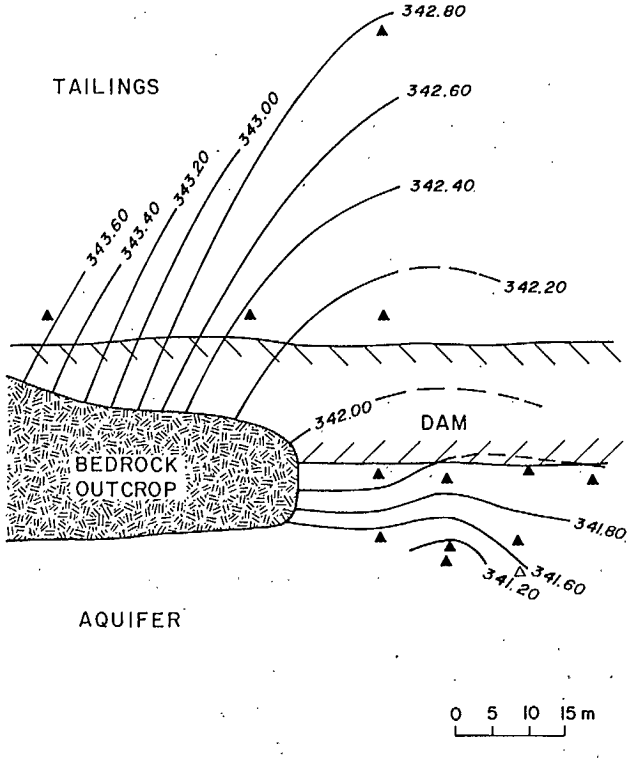

Fig. 5. Water table map of Seepage Area A for June, 1981. (Contour values are in meters above sea level.)

flow in the sand. In Seepage Area A, this drainage into the sand creates a strong horizontal gradient in the sand aquifer (Fig. 5). The gradient adjacent to the dam is approximately 0.050, decreasing to 0.020 about 30 m from the dam and to 0.005 about 100 m away. Employing the aforementioned porosity and conductivity, the average linear groundwater velocity near the dam is calculated to be about $500\,m\,yr^{-1}$. The borehole dilution test at WW1 (Fig. 4 and Morin and Cherry, 1988a) provided a more reliable in-situ measurement of $440\,m\,yr^{-1}$. Vertical gradients in the upper sand are generally less than the detection limit of 0.005.

In Seepage Area A, groundwater flowlines must converge as water flows around the bedrock knob to the west (Figs. 5 and 2.), which accounts for the shaped pattern. Nevertheless, both physical and chemical data (next section) indicate that bundle piezometers M1, M20, M8, M16, etc. (cross-section lines C-C′ and C-C″ on Fig. 4) generally define a flowline and mark the center of the acidic seepage plume. This demarcation of a flowline is emphasized so that chemical trends identified along the flowline are accepted as representing real attenuation processes. The two-dimensional vertical plane defined by the mini-piezometers along C-C′ is called the "centerplane" of the acidic plume.

4. CHEMICAL HYDROGEOLOGY OF SEEPAGE AREA A

In this section, the water chemistry, plume movement, and mineralogic composition of the sand are defined. The discussion of attenuation processes, specifically precipitation-dissolution of minerals, is presented in Section 5.

4.1 Water chemistry

Aqueous profiles along the vertical cross-section A-A′ (Fig. 4) indicate that an acidic plume with a core of approximately $3\,m^2$ cross-sectional area is flowing southward, slightly below the water table at M1 (Fig. 6). All ionic constituents in Table 1, except sodium, chloride, and silica, are at locally maximum concentrations in this plume. Aqueous profiles for cross-section B-B′ display trends similar to those of A-A′ with the plume centered at M8; however, concentrations in the center of the plume are lower at M8. These lower concentrations indicate contaminant attenuation processes are operating in Area A.

The attenuation of water-borne contaminants is more easily seen in profiles along the centerplane of the plume, C-C′ (Fig. 4). Cross-section C-C″ (the "far centerplane") allows the examination of relatively minor attenuation processes operating at greater distances from the impoundment (Morin, 1983, 1985), but are not discussed here.

Figures 7 through 10 show that the plume can be divided into three zones based on aqueous chemistry. The "inner core", which represents essentially unaltered acidic tailings seepage, has a pH < 4.8, Fe > 5000 ppm, and SO_4 > 11000 ppm. The "outer zone" has a pH > 5.5, Fe < 2500 ppm, and

pH (1980)

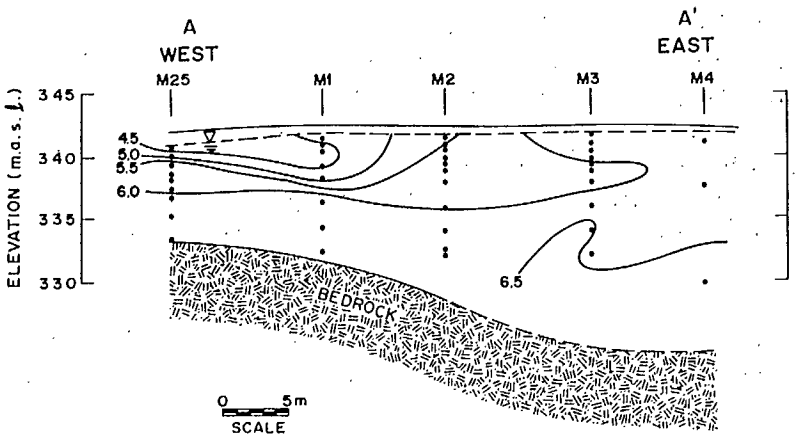

x 10^2 ppm IRON (1980)

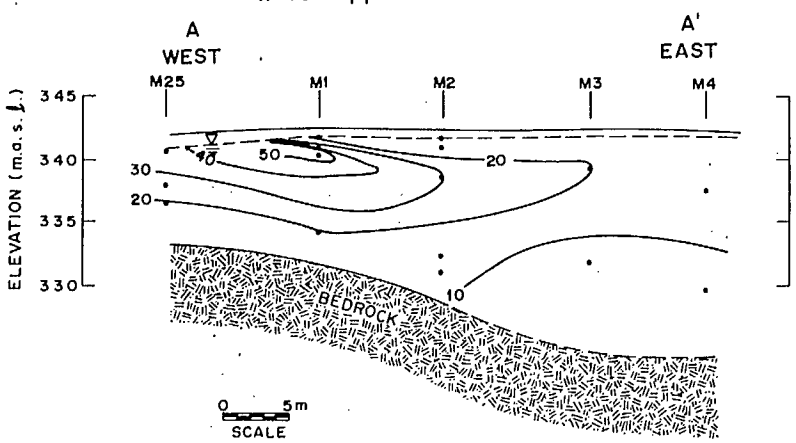

x 10^2 ppm SULFATE (1980)

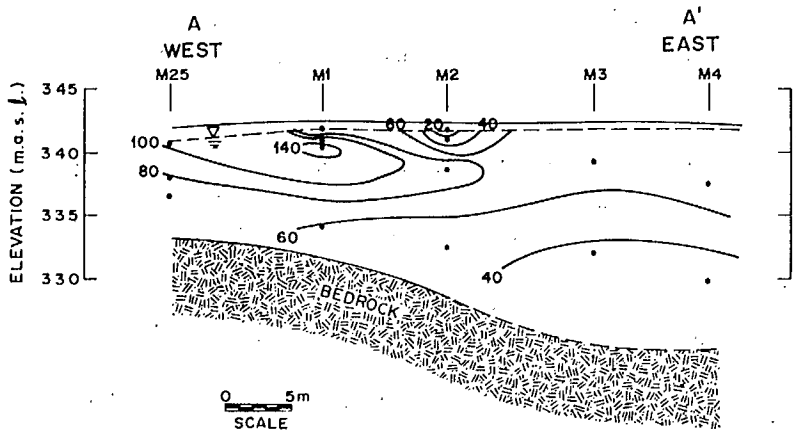

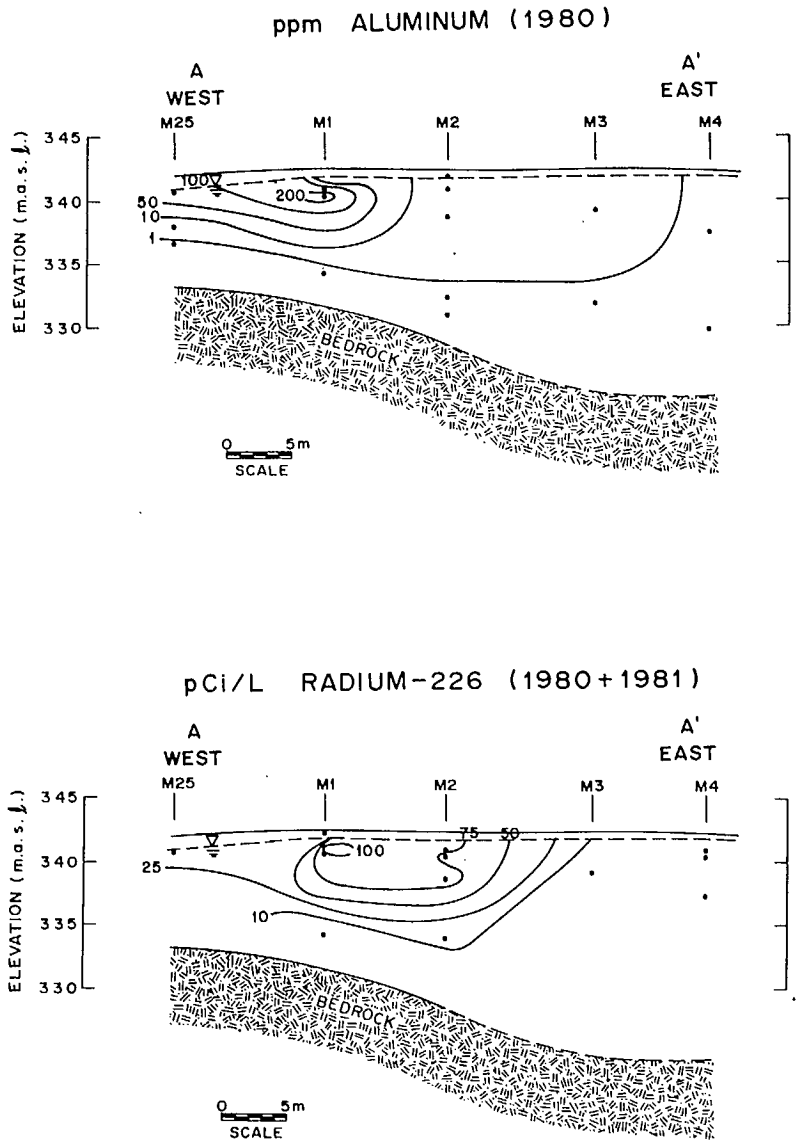

Fig. 6. Aqueous profiles along cross-section A-A'.

SO_4 < 7000 ppm. The outer zone contains both neutralized inner-core water near the water table and deeper pH-neutral mill-processing water still draining from the tailings. The transition region between the inner core and outer zone is called the "neutralization zone" in which pH is neutralized and concentrations of most elements decrease sharply. As will be shown in the third paper of this series (Morin and Cherry, 1988b), the neutralization zone itself is composed of "sub-regions". The neutralization zone surrounds the inner core like a sheath on all sides and its existence perpendicular to groundwater flow is attributed to transverse dispersion in the inner core and to the density contrast between the inner core and underlying outer zone. Although the inner-core and

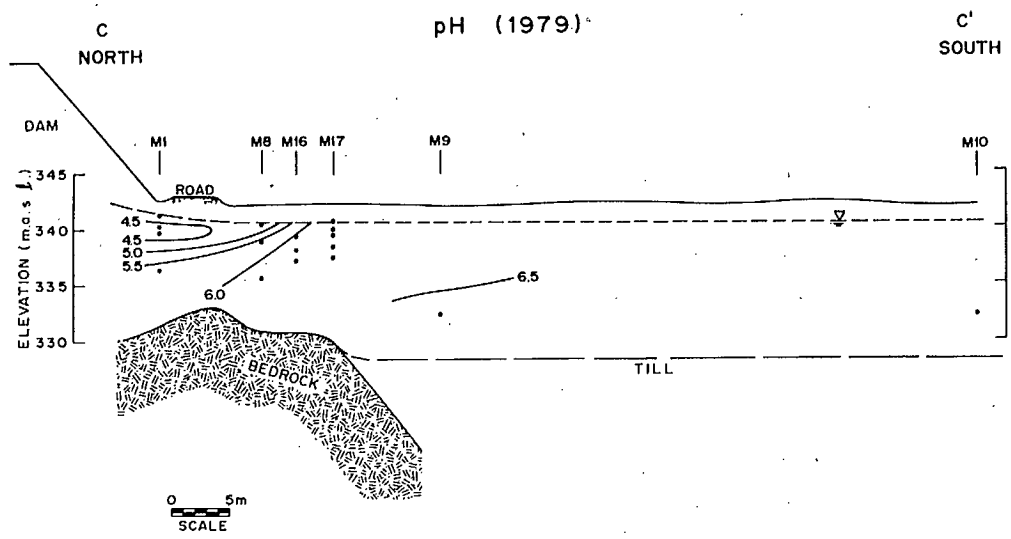
pH (1979)
C
NORTH
C'
SOUTH
DAM
M1
M8
M16
M17
M9
M10
ROAD
ELEVATION (m.a.s.l.)
345
340
335
330
4.5
4.5
5.0
5.5
6.0
6.5
BEDROCK
TILL
0
5m
SCALE

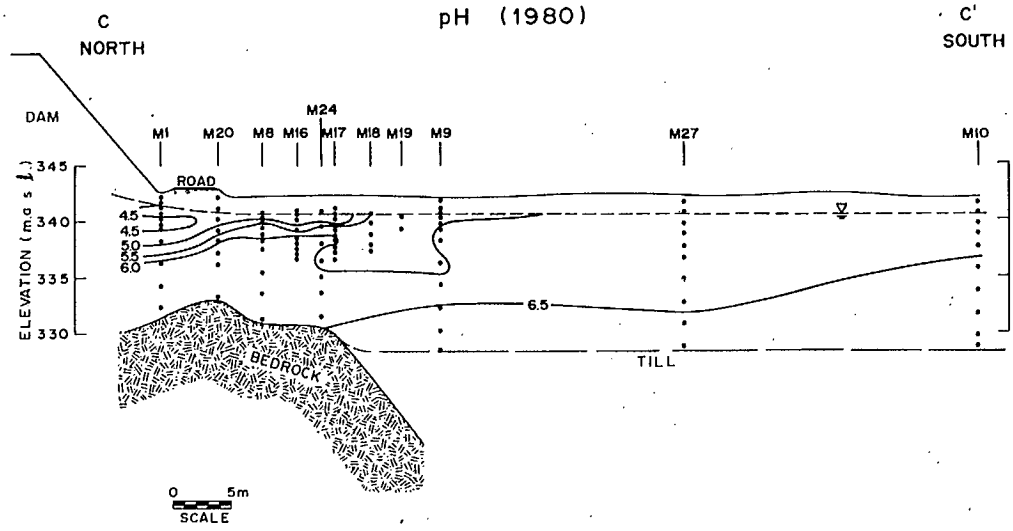
pH (1980)
C
NORTH
C'
SOUTH
DAM
M24
M1
M20
M8
M16
M17
M18
M19
M9
M27
M10
ROAD
ELEVATION (m.a.s.l.)
345
340
335
330
4.5
4.5
5.0
5.5
6.0
6.5
BEDROCK
TILL
0
5m
SCALE

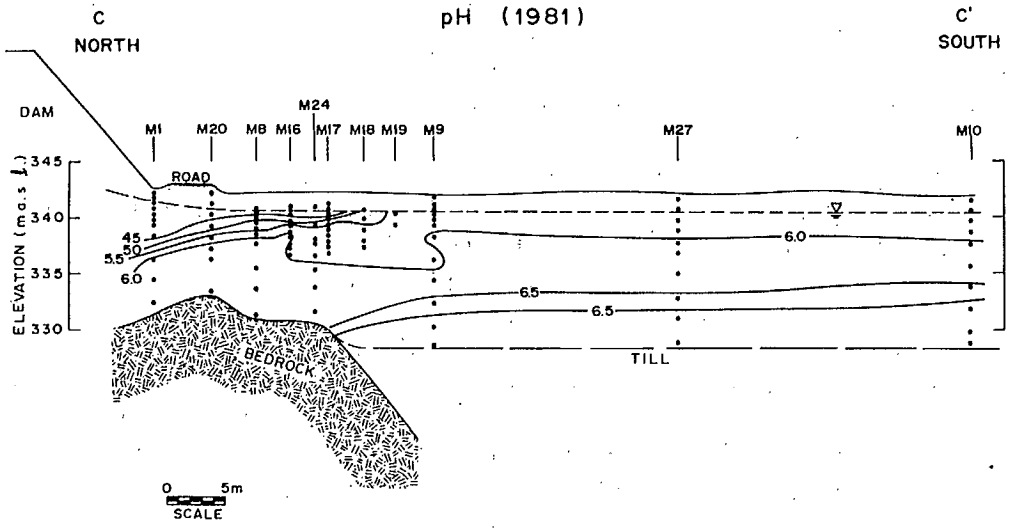
pH (1981)
C
NORTH
C'
SOUTH
DAM
M24
M1
M20
M8
M16
M17
M18
M19
M9
M27
M10
ROAD
ELEVATION (m.a.s.l.)
345
340
335
330
4.5
5.0
5.5
6.0
6.0
6.5
6.5
BEDROCK
TILL
0
5m
SCALE

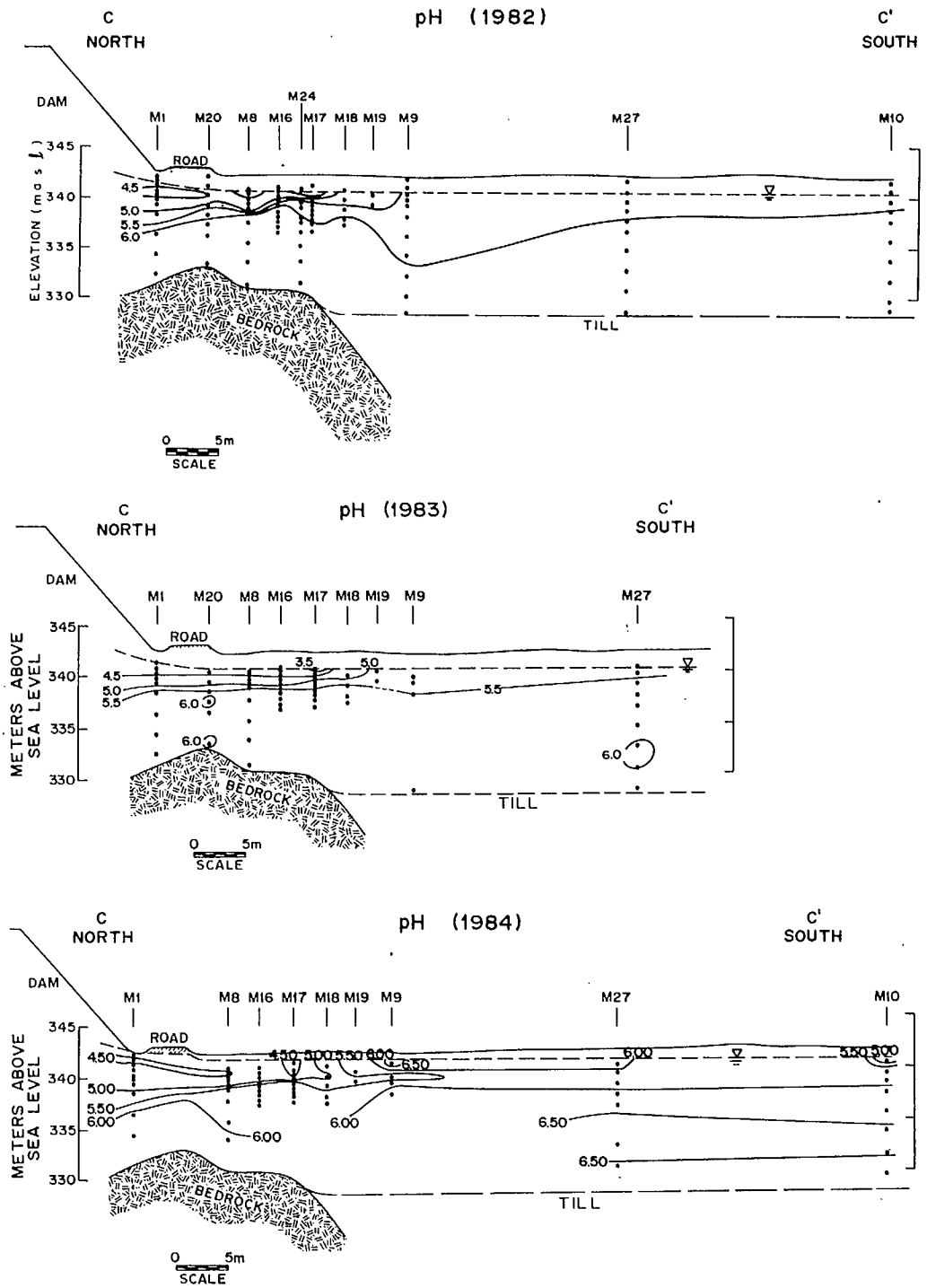

Fig. 7. pH profiles along the centerplane (cross-section C-C′).

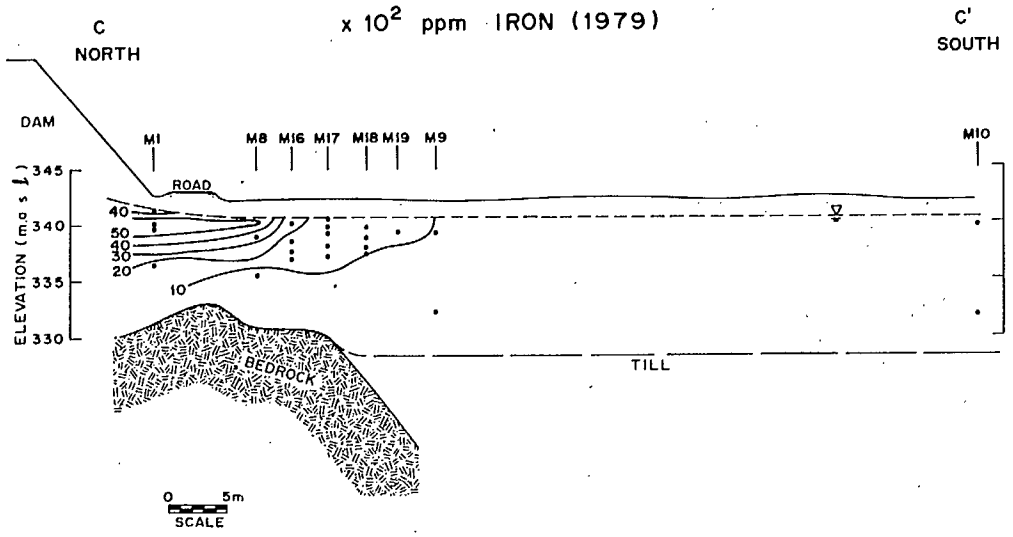
C
NORTH
x 10² ppm IRON (1979)
C'
SOUTH
DAM
M1
M8
M16
M17
M18
M19
M9
M10
ROAD
ELEVATION (mo s L.)
345
340
335
330
40
50
40
30
20
10
BEDROCK
TILL
0 5m
SCALE

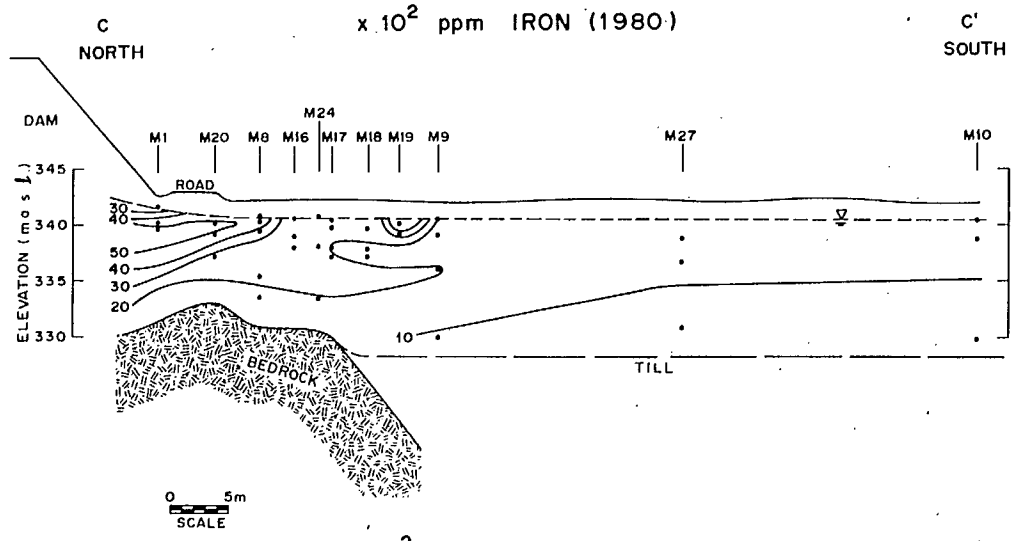
C
NORTH
x 10² ppm IRON (1980)
C'
SOUTH
DAM
M24
M1
M20
M8
M16
M17
M18
M19
M9
M27
M10
ROAD
ELEVATION (mo s L.)
345
340
335
330
30
40
50
40
30
20
10
BEDROCK
TILL
0 5m
SCALE

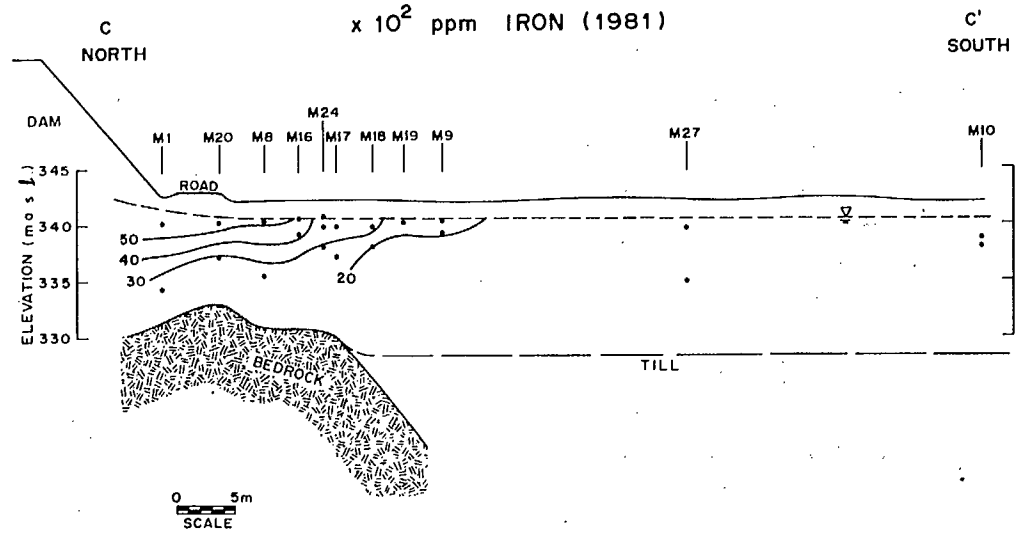
C
NORTH
x 10² ppm IRON (1981)
C'
SOUTH
DAM
M24
M1
M20
M8
M16
M17
M18
M19
M9
M27
M10
ROAD
ELEVATION (mo s L.)
345
340
335
330
50
40
30
20
BEDROCK
TILL
0 5m
SCALE

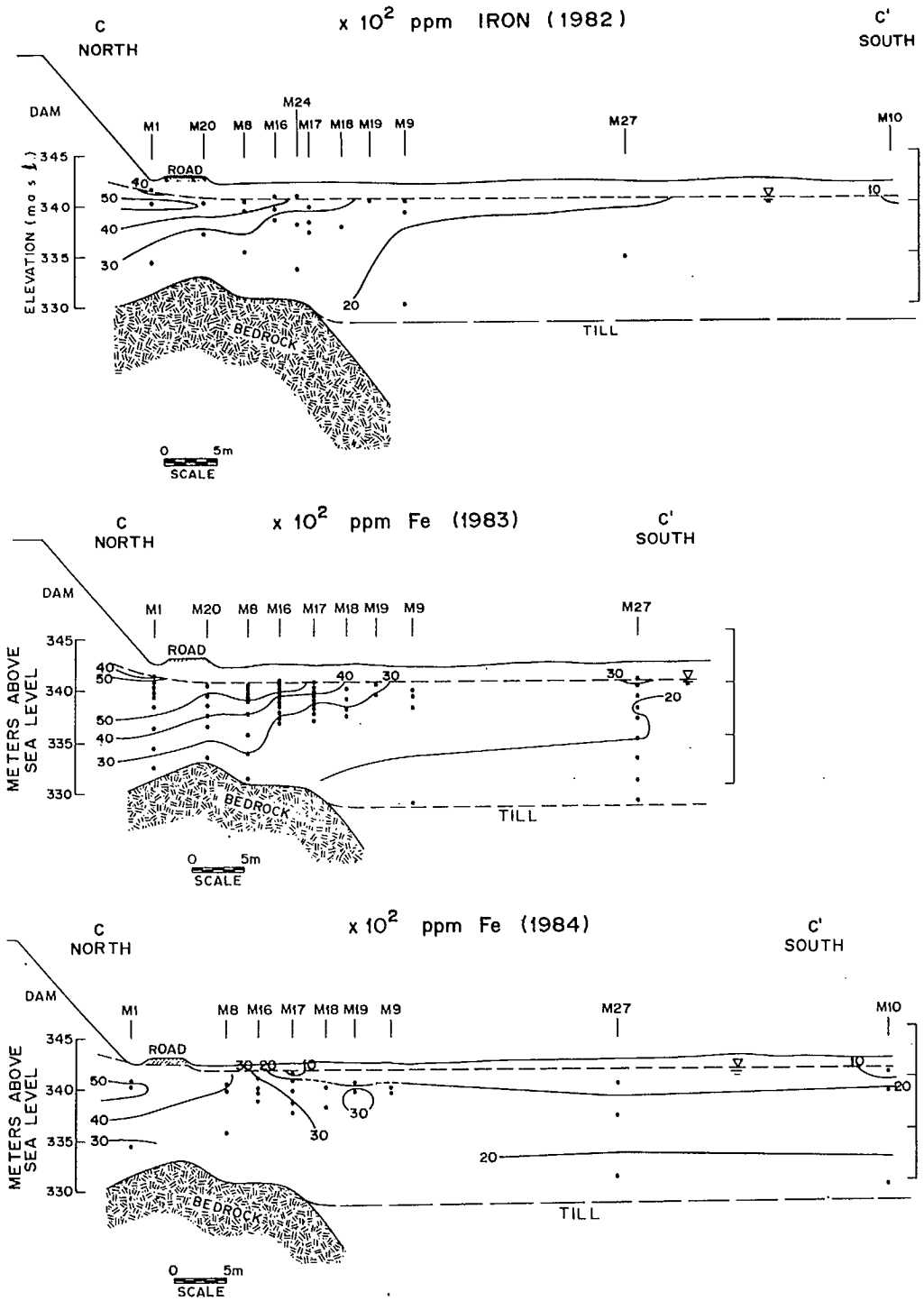

Fig. 8. Fe profiles along the centerplane.

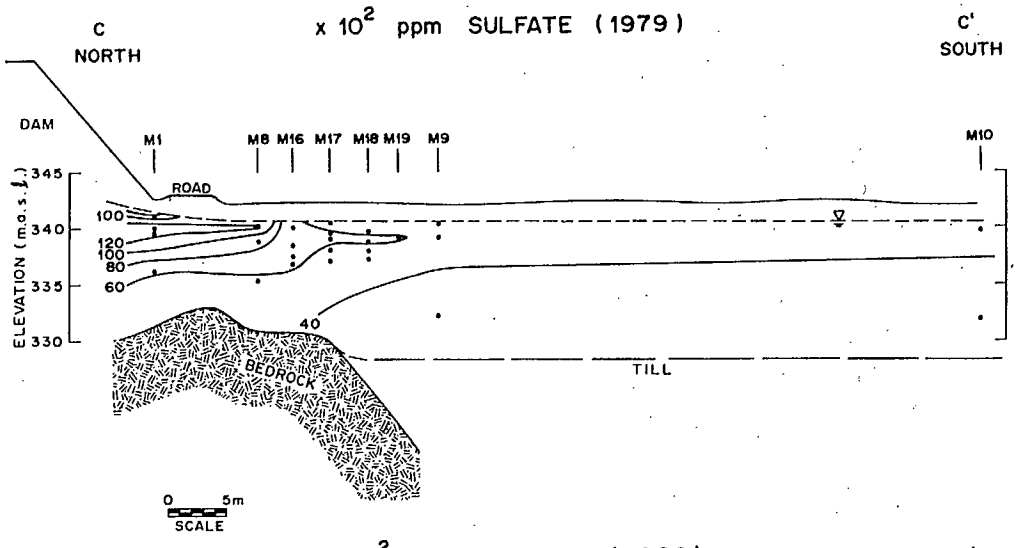
C
NORTH
x 10² ppm SULFATE (1979)
C'
SOUTH
DAM
M1
M8 M16 M17 M18 M19 M9
M10
ROAD
ELEVATION (m.a.s.l.)
345
340
335
330
100
120
100
80
60
40
BEDROCK
TILL
0 5m
SCALE

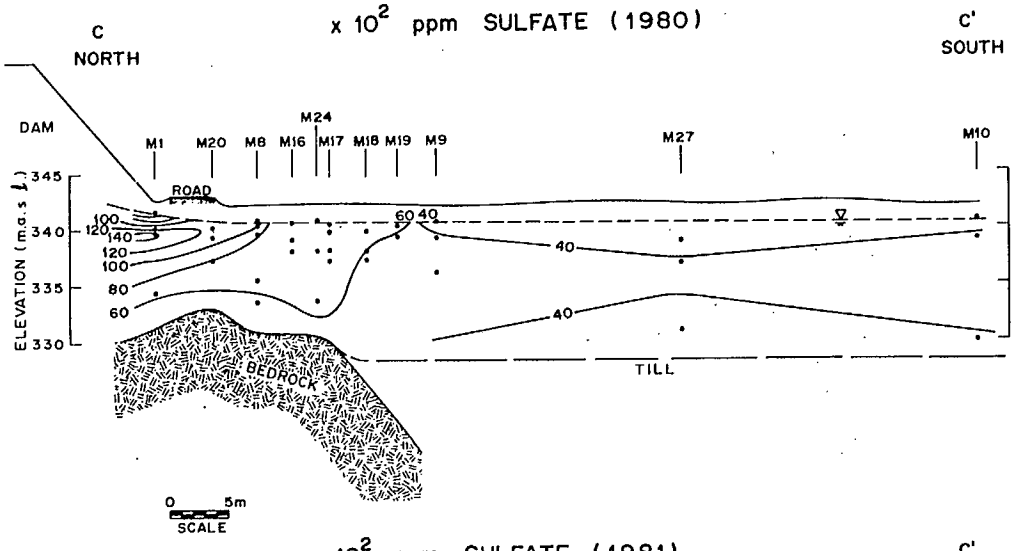
C
NORTH
x 10² ppm SULFATE (1980)
C'
SOUTH
DAM
M24
M1
M20
M8
M16
M17
M18
M19
M9
M27
M10
ROAD
ELEVATION (m.a.s.l.)
345
340
335
330
100
120
140
120
100
80
60
60
40
40
40
BEDROCK
TILL
0 5m
SCALE

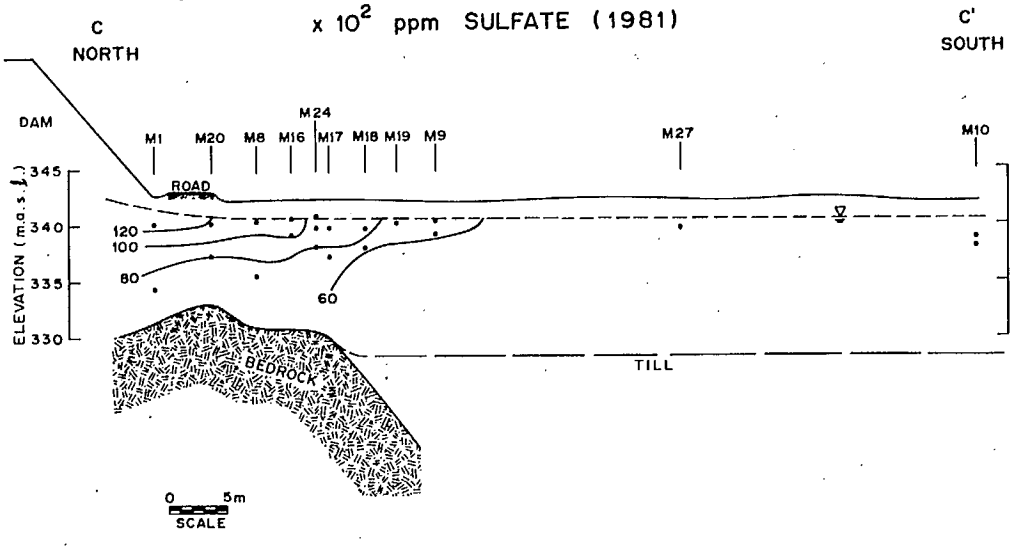
C
NORTH
x 10² ppm SULFATE (1981)
C'
SOUTH
DAM
M24
M1
M20
M8
M16
M17
M18
M19
M9
M27
M10
ROAD
ELEVATION (m.a.s.l.)
345
340
335
330
120
100
80
60
BEDROCK
TILL
0 5m
SCALE

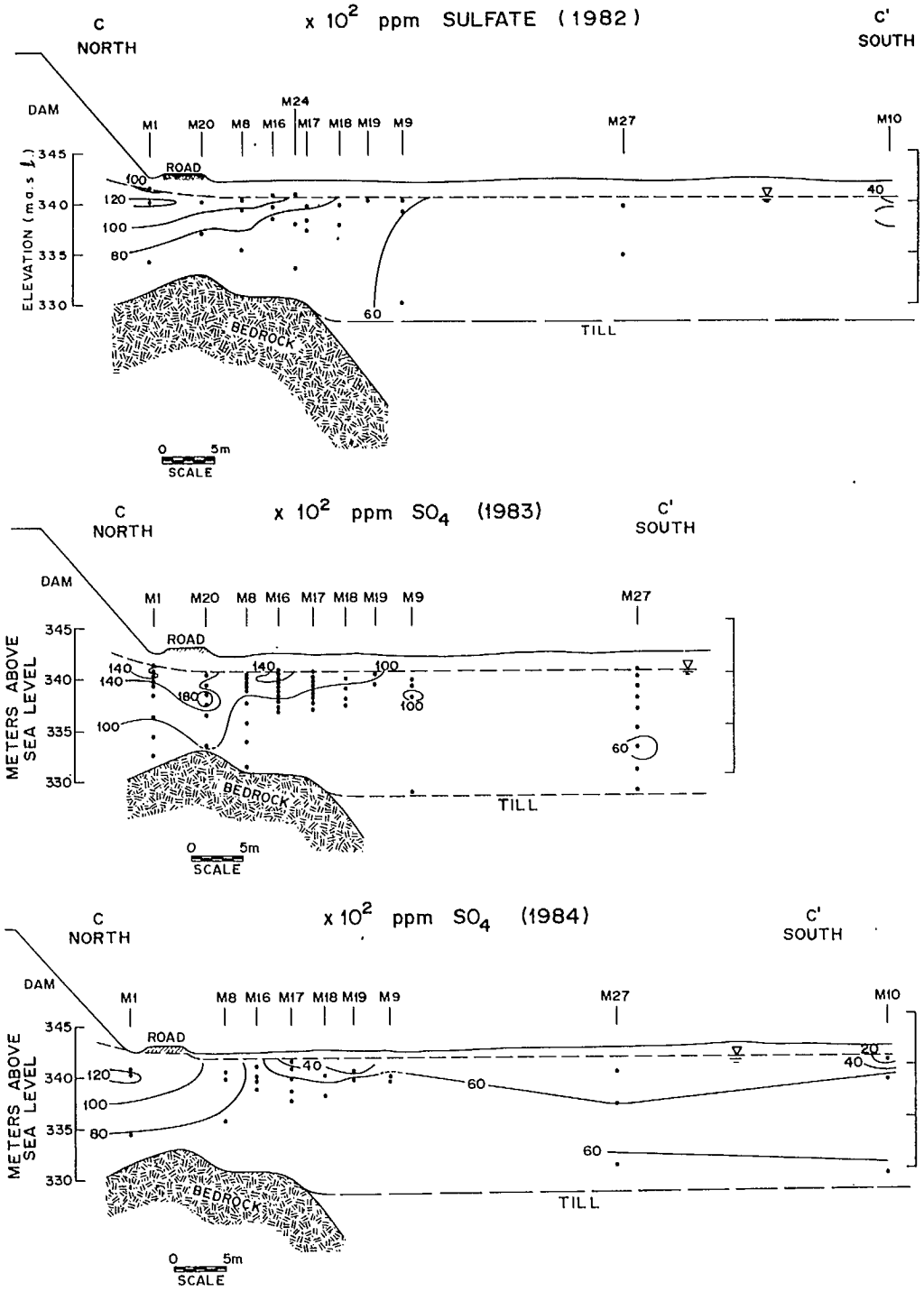

Fig. 9. Sulfate profiles along the centerplane.

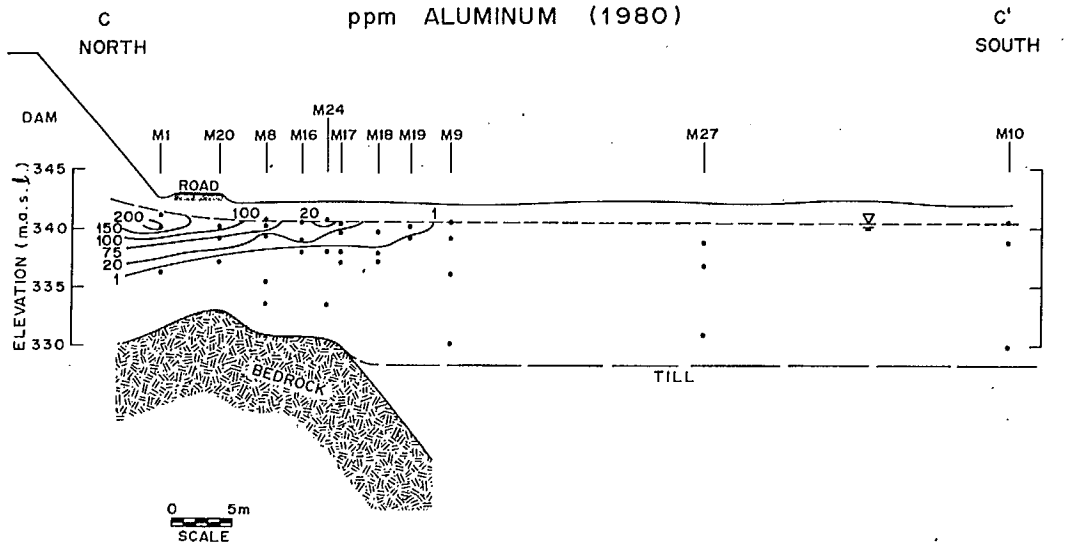

Fig. 10. Aluminum profile along the centerplane.

neutralized inner-core water are denser than underlying process water, the inverse density stratification persists to the edge of the monitoring network, hundreds of meters and several years away.

Unsuccessful attempts were made to locate the source area of the plume within the tailings mass through piezometer installation and monitoring (T8 series and M36 and M37 in Fig. 4). Because the plume is near the water table in Area A, a simple flownet analysis suggests the source area is probably close or adjacent to the dam and flux calculations indicate the lateral extent of the source area could be as small as $9\,m^2$. Simulations with the chemical-equilibrium computer programs (third paper of this series: Morin and Cherry, 1988b), based on the conceptual model developed in this paper, also indicate the source area is probably adjacent to or within the dam north of M1. This location appears reasonable in that the coarse-fill dam may allow significant amounts of oxygen and precipitation to contact laterally adjacent tailings. This type of "local acid anomaly" demonstrates the inherent limitation of defining an entire tailings pile as either acidic or pH-neutral.

4.2 Plume movement

In order to detect average yearly movement of the inner core and neutralization zone, fifty to one hundred samples were collected over a period of a few days each summer from 1979 to 1982. In the summer of 1983, samples were collected from every centerplane piezometer. In 1984, fifty samples plus replicates were collected in November.

To facilitate detection of movement, one-dimensional profiles along the plume's axis (the "centerline") were produced (Fig. 11). The mini-piezometer in each centerplane bundle that had the lowest pH and the highest specific

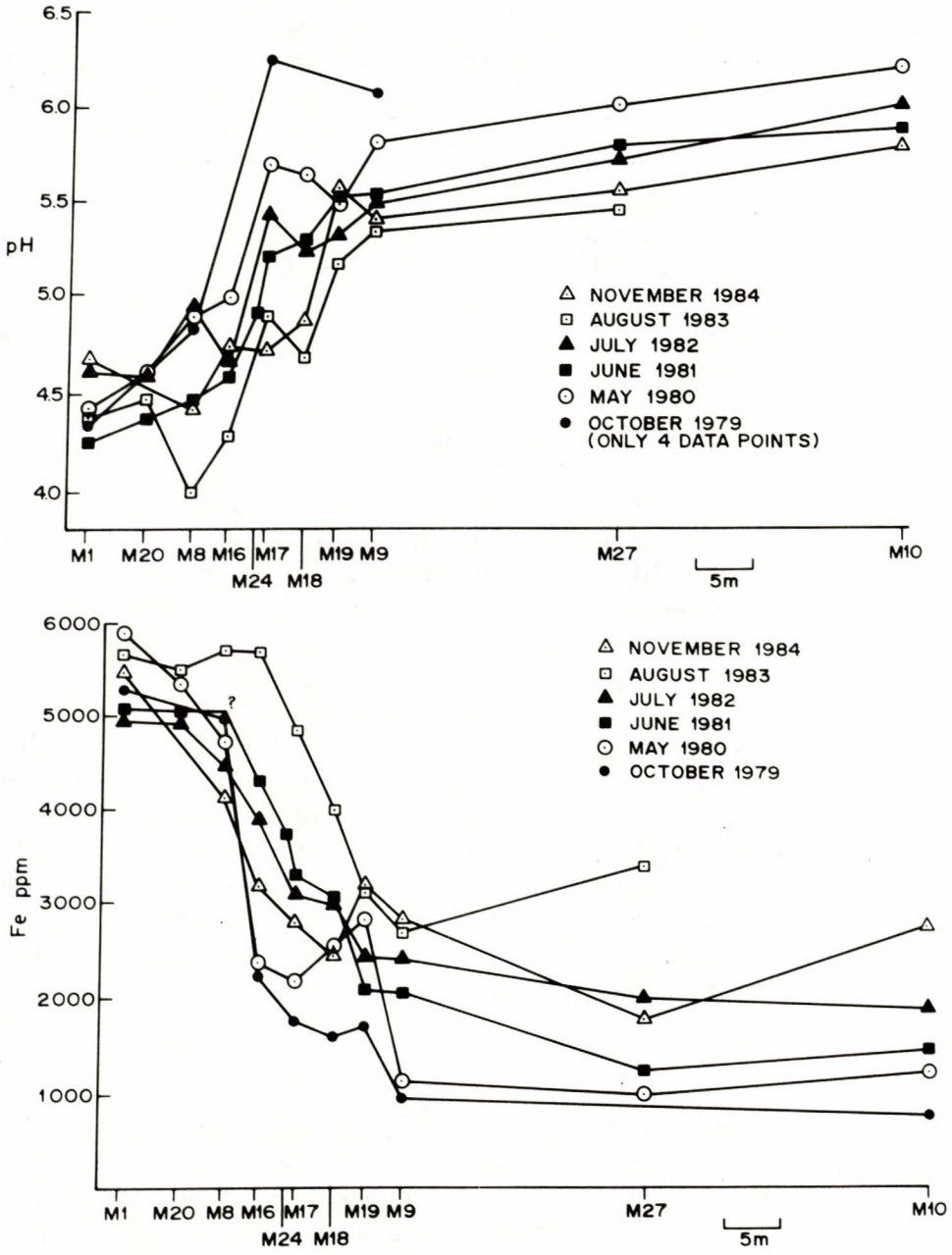

Fig. 11. Aqueous profiles along the one-dimensional centerline.

conductance marks the centerline, but because of limitations in one-dimensional profiles in Area A (Morin, 1985) centerline profiles must be used in conjunction with centerplane profiles to determine movement quantitatively. Figures 7 through 11 indicate the contact of the inner core and neutralization zone is migrating about 1–2 m annually and the contact of the neutralization zone and outer zone is migrating about 10 m annually. A smooth yearly progression is

not apparent because of (1) the bundle piezometer spacing of greater than 2.5 m, (2) temporal fluctuations in input concentrations from the source area, and (3) possible temporal variations in the geochemical processes regulating aqueous concentrations. Additionally, iron profiles for 1984 imply a retrograde (upgradient) movement; however, aqueous iron is regulated by siderite formation and the yearly saturation-index profiles for siderite do not display this retrograde movement (discussed further in Section 5.3).

Because average linear groundwater velocity near the dam in Area A is about $440\,m\,yr^{-1}$, migration rates of 1–2 and $10\,m\,yr^{-1}$ represent significant retardation of contaminant migration. The geochemical processes accounting for this retardation are defined in Section 5.

4.3 Mineralogic composition of the sand aquifer.

The sands consist predominately of quartz and feldspars with some pyroxene, amphibole, and magnetite (Morin, 1983). These minerals are relatively stable and, thus, likely have no significant effect on contaminant migration. Furthermore, because aluminum is precipitating from solution in the neutralization zone (Section 5.5), the complex scenario of feldspar dissolution can be ignored in this zone.

Trace amounts (< 1 wt. %) of relatively reactive minerals also exist in the sand, but are below the detection limits of most methods. Although trace levels of minerals may appear relatively unimportant, Morin and Cherry (1986) show that trace amounts can have a major impact on contaminant migration. Trace minerals apparently present in the sand are: calcite (an average of 0.86 wt. % in the lower sand), siderite (particularly in the upper sand where calcite is converted to siderite), gypsum, and Al-OH minerals (discussed further in the following section). In addition, a few radionuclide minerals may exist in the sand (see second paper of series: Morin et al., 1988).

5. INTERACTIONS OF SOLID AND LIQUID PHASES

The significant retardation of major ions, metals, and radionuclides with respect to groundwater movement is the result of solute transfer from the aqueous phase to the aquifer matrix, although the removed species are eventually remobilized to a lesser degree. This phase interaction is regulated by the geochemical processes of mineral precipitation-dissolution, co-precipitation with minerals, and ion exchange (sorption). However, because of the low cation-exchange capacity (CEC) of the sand of approximately 0.6 meq/100 g and because of the high aqueous concentrations relative to the CEC, the effect of ion exchange is limited. Additionally, because of active mineral precipitation in the neutralization zone, it is not always possible to distinguish between co-precipitation and adsorption onto precipitating minerals of minor species. As a result, ion exchange and sorption have been eliminated from the quantitative analysis. Equilibrium and metastable approaches to the geochemical processes are considered acceptable here, because relatively high concentra-

tions of most species in Area A should provide a strong driving force towards equilibrium.

The physico-chemical process of hydrodynamic dispersion would normally be significant at sites such as Area A with fast groundwater velocities and strong concentration gradients between the geochemical zones. However, because the concentrations of many solutes are strongly regulated by specific geochemical processes in each zone in Area A, the solutes are transferred to the solid phase as they are dispersed into a downgradient zone. As examples, hydronium irons (represented as H^+ in this study for simplicity) in the inner core are neutralized as they enter the neutralization zone, and iron in the inner core forms siderite as it disperses into the neutralization zone. As a result, the effect of dispersion of temporally decreasing concentration gradients is largely overcome by the maintenance of concentration gradients by neutralization and precipitation in adjacent geochemical zones.

For ease of understanding, the conceptual model of contaminant migration is first summarized in the following subsection and facets of the model are then discussed in terms of data from Area A in subsequent subsections. It is important to note that this conceptual model is general in nature because it has been developed from studies of several acidic uranium-tailings sites across North America (see third paper of series: Morin and Cherry, 1988b) as well as from acid-drainage studies.

5.1 Conceptual model of contaminant migration

Within the source area of the plume in the tailings mass, infiltrating precipitation and gaseous and dissolved oxygen oxidize pyrite. The oxidation process involves a number of reaction steps, but the overall reaction can be described as:

$$2FeS_{2(s)} + 2H_2O + 7O_{2(g)} \leftrightarrow 2Fe^{2+} + 4H^+ + 4SO_4^{2-} \quad (1)$$

Pyrite oxidation continuously provides high concentrations of sulfate, iron, and H^+ to the tailings pore water. Because the solubilities of some compounds increase and the sorptive capacity of solids for cations decreases as the pH drops from neutral to acidic values, a decline in pH causes the release of many metals and radionuclides from the tailings solids to the pore water. Thus, pH is a major control on the aqueous behavior of many ions. Evidence for this scenario operating in the Nordic Main tailings is presented in Cherry et al. (1980), Davé et al. (1981), Smyth (1981), Dubrovsky et al. (1984), and Dubrovsky (1986).

Because pyrite oxidation at Nordic Main probably began in the late 1960's as the ponded surface water was drained, contaminated acidic groundwater (inner-core water) began many years ago to enter the aquifer at the impoundment dam. For convenience in explaining the following geochemical processes in the aquifer, the acidic water is envisioned as travelling along the centerline in Area A through a streamtube. This streamtube is divided into a series of cells in which various geochemical reactions occur as the groundwater advances.

Although a number of reactions are capable of explaining individual trends, the following suite of interrelated reactions satisfactorily explains all trends.

When inner-core water enters a cell for the first time, the pH is raised towards neutral values by dissolution of calcite:

$$2H^+ + CaCO_{3(s)} \leftrightarrow Ca^{2+} + H_2CO_3^0 \quad (2)$$

and

$$H^+ + CaCO_{3(s)} \leftrightarrow Ca^{2+} + HCO_3^- \quad (3)$$

If solution pH remains below 6.45 (at temperatures near 10°C), reaction 2 is the dominant reaction.

As the pH rises, iron is removed from solution by the precipitation of an iron compound. The two most likely minerals are siderite ($FeCO_3$), which forms with Fe^{2+}, and iron hydroxide ($Fe(OH)_3$), which forms with Fe^{3+}. Many of the following precipitation reactions are written with Fe^{2+}, because high aqueous iron concentrations at near-neutral pH predominately occur in the 2^+ state:

$$Fe^{2+} + H_2CO_3^0 \leftrightarrow FeCO_{3(s)} + 2H^+ \quad (4)$$

$$Fe^{2+} + HCO_3^- \leftrightarrow FeCO_{3(s)} + H^+ \quad (5)$$

$$Fe^{2+} + CO_3^{2-} \leftrightarrow FeCO_{3(s)} \quad (6)$$

$$Fe^{3+} + 3H_2O \leftrightarrow Fe(OH)_{3(s)} + 3H^+ \quad (7)$$

$$Fe^{2+} + 3H_2O + X \leftrightarrow Fe(OH)_{3(s)} + 3H^+ + Y \quad (8)$$

where X and Y are a redox couple that provide the necessary electron transfer for the valence-state change of iron. The stoichiometric coefficients of reaction 8 vary with the particular redox couple replacing X and Y. For example, where oxygen is involved, one possible reaction is:

$$4Fe^{2+} + 10H_2O + O_{2(g)} \leftrightarrow 4Fe(OH)_{3(s)} + 8H^+ \quad (9)$$

Amorphous $Fe(OH)_3$ is considered the ferric-oxide mineral most likely to precipitate, although related minerals such as goethite (α-FeOOH) may precipitate with or in place of $Fe(OH)_3$ (e.g., Langmuir and Whittemore 1971; Sung and Morgan, 1980).

Where sufficient calcite exists in the solid matrix and siderite is capable of precipitation, the precipitation reaction actually becomes a mineral-replacement reaction because of the calcite-siderite solid solution (Morin and Cherry, 1986):

$$Fe^{2+} + CaCO_{3(s)} \leftrightarrow FeCO_{3(s)} + Ca^{2+} \quad (10)$$

Reaction 10 produces no H^+ and does not significantly affect concentrations of DIC, unlike previous equations. Because there is a solid-solution series or significant substitution among the carbonates of Ca, Fe, Mg, Mn, Zn, Co, and Cd (e.g. Goldsmith, 1959; Lippman, 1980), the aqueous concentrations of these

ions are capable of being regulated by the precipitation-dissolution of calcite-siderite in Area A.

Sulfate concentrations are typically high in acidic tailings porewater and seepage, and the waters are often near saturation with respect to gypsum. Therefore, as calcite dissolves in a cell (reactions 2, 3, or 10), the addition of calcium ions to the groundwater causes gypsum supersaturation and precipitation:

$$Ca^{2+} + SO_4^{2-} + 2H_2O \leftrightarrow CaSO_4.2H_2O \quad (11)$$

As a result, a large increase in aqueous calcium along the streamtube is not observed.

As the pH in the aquifer cell increases, supersaturation with respect to minerals containing aluminum and/or silica often occurs. The most likely minerals to precipitate are $Al(OH)_3$:

$$Al^{3+} + 3H_2O \leftrightarrow Al(OH)_{3(s)} + 3H^+ \quad (12)$$

amorphous silica or quartz:

$$H_4SiO_4^0 \leftrightarrow SiO_{2(s)} + 2H_2O \quad (13)$$

and amorphous allophane of variable composition (Paces, 1973, 1978).

As the pH increases and minerals precipitate, the adsorption, precipitation, or co-precipitation of other metals and radionuclides also occur.

As low-pH water continuously enters a cell and is neutralized, eventually all of the calcite in the cell is consumed. At this point, a lower pH then exists in the cell and low-pH water then begins to flow into the next downgradient cell in the streamtube. In this next cell, the aforementioned reactions occur again until all calcite is dissolved. In this way, a migration of acidic inner-core water is retarded and attenuated. In cells where all calcite has been removed, the precipitates redissolve in response to the presence of inner-core water in the cell. For example, the dissolution of siderite (reverse of reaction 4) neutralizes pH as does calcite, but to a lesser degree because of the lower solubility product of siderite and the often high aqueous concentrations of ferrous iron relative to calcium. In effect, this redissolution in upgradient cells partially neutralizes the inner-core water so that relatively little calcite has to dissolve in downgradient cells to fully neutralize the water and this fact indicates retardation is more complex than the simple calcite scenario (Morin and Cherry, 1988b). The following subsections examine the specific reactions of the conceptual model as applied to the field study in Seepage Area A.

5.2 Calcite

Auger samples of aquifer material were analyzed for trace amounts of solid carbonate by the method of Barker and Chatten (1982), which apparently does not differentiate among calcite, dolomite, siderite, and other carbonates. The

detection limit of the method is about 0.002 wt. % calcite and, based on three replicates, precision is within 3% of the reported value.

Within the inner core, carbonate analyses yield < 0.002 wt.% as expected. Analyses indicate < 0.002 to 0.04 wt. % exists in the outer zone within the upper sand, where a significant portion of the carbonate probably exists as siderite because of relatively high iron concentrations. For the lower sand (outer zone) where iron concentrations are lower, results of analyses range from 0.31 to > 1.4 wt. % in general agreement with thin-section analysis. The disagreement in carbonate content of the outer zone between the upper and lower sands is believed to be due to a sampling problem. Upon sampling the outer zone in the upper sand, the oxidation and precipitation of aqueous iron (reaction 9) could remove up to 0.2 wt. % of solid carbonate and any remaining siderite could convert to $Fe(OH)_3$ by oxidation. In light of this problem, the initial carbonate content of the entire outer zone is assumed to be 0.3 to 1.4wt. % with an average content of 0.85 wt. % for quantitative purposes.

Returning to the aquifer cell-and-streamtube concept, the cross-sectional area of the streamtube is arbitrarily set at $1\,m^2$ and the streamtube is partitioned into cells of 1 m length. Because the porosity of the upper sand is about 36%, a 1-m^3 cell contains $0.36\,m^3$ (360 L) of groundwater and $0.64\,m^3$ of sand. Because the specific gravity of the upper sand is 2.98, there is about 1.9×10^6 g of sand in each cell. A cell therefore initially contains an average of 162 moles (1.62×10^4 g) of calcite based on an average of 0.85 wt. %; the actual value is likely in the range of 57 to 266 moles per cell (0.31–1.4 wt. %). Because the pH of inner-core water is about 4.5, one cell (360 L) contains 0.011 moles of H^+. By reactions 2 and 3, 162 moles of calcite would neutralize 162–324 moles of H^+. As a result, 14700–29500 pore volumes (162/0.011 to 324/0.011) must pass through a cell to remove all calcite, and the retardation coefficient would be between 0.000067 (0.011/163) and 0.000034 (0.011/325) of groundwater velocity. This retardation coefficient is about 2 orders of magnitude smaller in value than the observed value of almost 0.003 for the pH front in the pH range 5.0 to 5.2. Therefore, there must be another major processes consuming calcite.

5.3 Iron precipitation

The conceptual model holds that iron precipitates from solution as either siderite (reactions 4, 5, 6, or 10) or $Fe(OH)_3$ (reactions 7, 8, or 9). Because all the iron reactions produce significant amounts of acidity except reaction 10 and involve either Fe^{2+} or Fe^{3+}, it is important to establish which reaction applies so that calculations can be made on pH neutralization and redox conditions.

Several methods were employed to determine which iron mineral is precipitating in Area A. These methods are explained in detail in Morin and Cherry (1986) and are summarized here. Firstly, measurements of pH and Eh were plotted on a pH-Eh-Fe stability diagram (Fig. 12), which indicates that siderite is a stable iron mineral. Problems associated with Eh measurements in Area A and limitations in pH-Eh diagrams are discussed in Morin (1983, 1986). Secondly, speciation of the water and calculation of mineral saturation indices

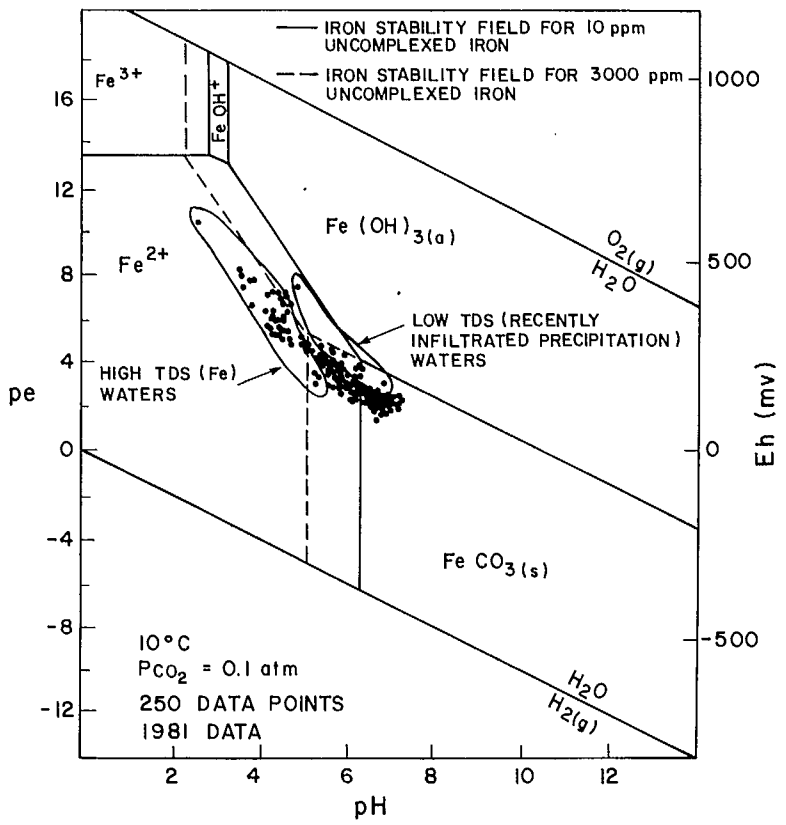

Fig. 12. pH-Eh-Fe stability diagram.

(SI = ion activity product/equilibrium constant at solution temperature) by the WATEQ2 program (Ball et al., 1979) provided log SI siderite values for the centerplane (Fig. 13). These values are near or above saturation in much of the neutralization and outer zones. The solubility of ferric-oxide minerals in Area A is presented as pQ in Fig. 14, where $pQ = -\log_{10} [Fe^{3+}][OH^-]^3$ at 25°C (Langmuir and Whittemore, 1971; Whittemore and Langmuir, 1975). Figure 14 indicates probably little ferric iron is precipitating in the inner core and neutralization zone of Area A.

Thirdly, the stoichiometry of Equation 8, which would be the valid reaction if significant amounts of iron were precipitating as $Fe(OH)_3$ in Area A, indicates $Fe(OH)_3$ precipitation is dependent on the redox couple, X-Y. Morin (1983) evaluated four redox couples and concluded that these couples would only allow a maximum of a few tens of ppm iron to precipitate as $Fe(OH)_3$ in Area A. Also, because Eh changes through the neutralization zone are relatively minor (pH 4.8–5.5 on Fig. 12), little oxidation of Fe^{2+} to Fe^{3+} can be occurring. Furthermore, if the 3500 ppm iron that is lost through the neutralization zone precipitated as $Fe(OH)_3$, the amount of calcite that would have to dissolve to account for the observed neutralization would produce an increase in DIC of about 0.1 molal. However, DIC values do not rise above

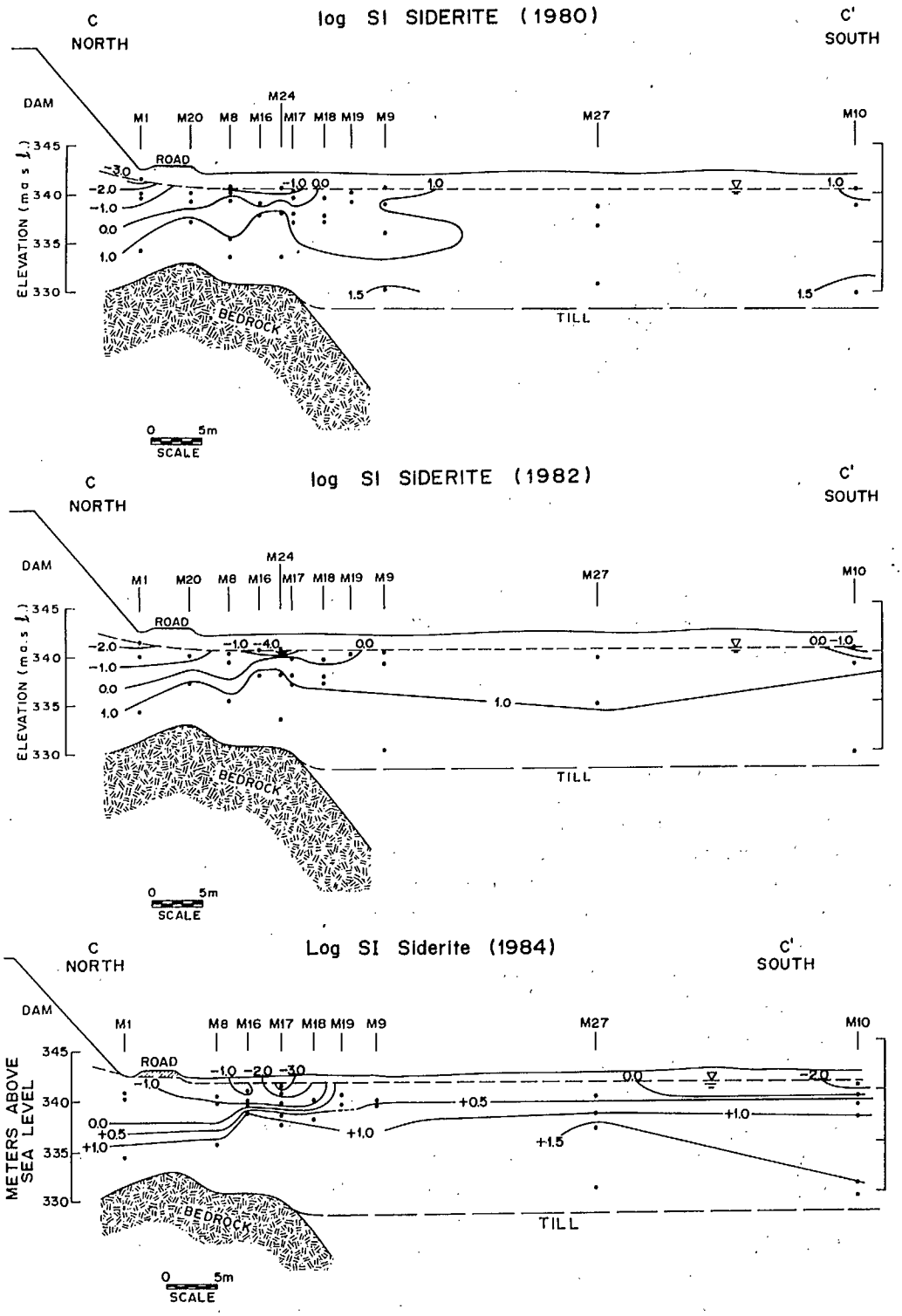

Fig. 13. Log SI siderite for the centerplane.

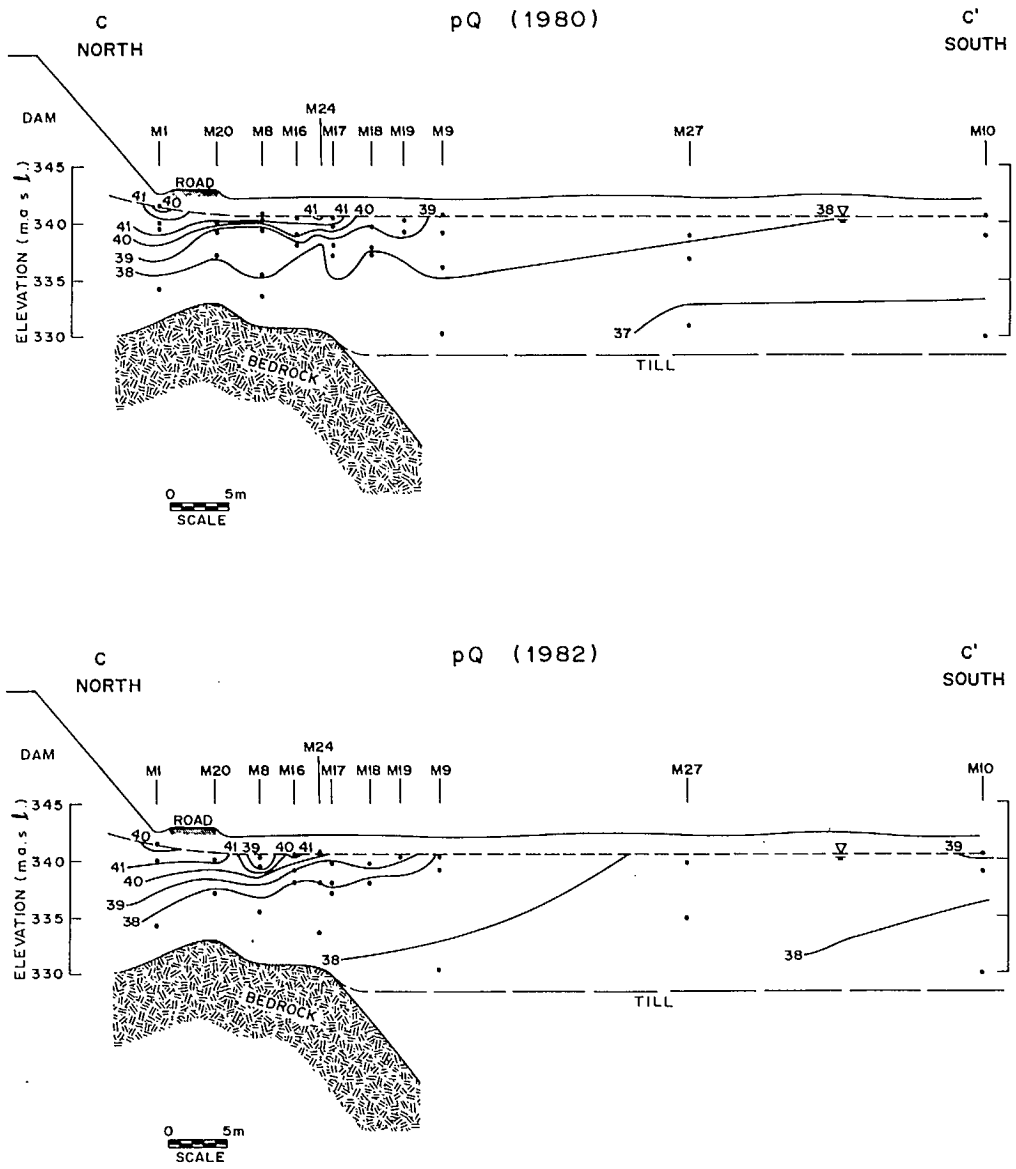

Fig. 14. pQ diagrams for the centerplane.

approximately 0.01 molal in Area A. Therefore, only minimal quantities of ferric-iron minerals are probably precipitating in most of Area A.

Through the inner core and part of the neutralization zone, log SI siderite (Fig. 13) is less than 0.0, indicating the instability and probable absence of siderite. Through the remainder of the neutralization zone and outer zone, log SI siderite varies from saturation to significant supersaturation, indicating siderite is probably forming as aqueous iron decreases in these regions. The presence of calcite indicates reaction 10 probably describes the net precipitation reaction in these regions.

Returning to the cell-and-streamtube concept, a total of about 3500 ppm iron is lost apparently by conversion of calcite to siderite through the neutralization zone along a flow distance of about 5 m (5 cells), or about 4.42 moles per 1-m^3 cell. Because aqueous iron concentrations are higher than those of calcium and the solubility of siderite is much lower than that of calcite, the formation of siderite essentially removes much of the neutralization capacity of the carbonate. Therefore, because a cell initially contains 162 moles of calcite, it would require about 37 pore volumes (162/4.42) to totally convert the calcite, and the resulting retardation coefficient is 4.42/163 or 0.027 of groundwater velocity. Because pH is neutralized at the same time as siderite is forming (Section 5.2), the total amount of calcite removed per pore volume is actually $4.42 \pm 0.011 = 4.43$ excluding aqueous buffering reactions. This summation demonstrates the minor effect that simple pH neutralization can have on migration rates. The value of 0.027 is only one order-of-magnitude larger in value than the observed retardation of 0.003, whereas the simple pH-neutralization value was 0.000035–0.000067 is roughly two orders-of-magnitude smaller. The explanation for the one order-of-magnitude difference (0.027–0.003) is that subsequent redissolution of the precipitated minerals contribute to retardation. The redissolution and aqueous buffering reactions are too numerous and complex for cell-and-streamtube calculations and, thus, computer programs were written to simulate the conceptual model (Morin and Cherry, 1988b).

In Section 4, it was pointed out that the 1984 iron profile displayed anomalous retrograde movement relative to previous years (Figs. 8 and 11). However, log SI siderite trends (Fig. 13) theoretically should not and do not display the retrograde movement. This situation highlights the potential error in examining single-ion contaminant migration in systems regulated by mineral solubility.

5.4 Gypsum

There are apparently no reported problems in the nucleation and precipitation of gypsum and, thus, groundwater should exhibit a log SI value near 0.0 wherever gypsum is precipitating or dissolving. The groundwaters in Area A are in equilibrium with gypsum (log SI = 0.0 to +0.15) along most of the centerplane. Because sulfate concentrations decrease along the centerline, gypsum is probably precipitating where calcium is added to solution during calcite replacement.

Because there is 5500 ppm sulfate lost through the neutralization zone over a length of about 5 m, there are 4.13 moles of gypsum (calcium and sulfate) precipitated per 1-m^3 cell. This value must also represent the amount of calcium added to solution (then quickly lost to gypsum) and the amount of iron lost (4.42 moles per cell) by siderite replacement. Therefore, mass balance is generally maintained within the model.

As indicated by calculations above, gypsum should occur in solid-phase

concentrations similar to those of calcite and siderite (< 1 wt. %). The wt. % sulfate curve for a core taken 5 m west of piezometer M8 (Morin et al., 1982) indicates negligible sulfate exists in the sand. However, total sulfur analyses for the core yielded values of about 0.1–0.2 wt. %, which is the approximate amount of gypsum expected. Because the only known source of sulfur in the sand is gypsum, it is not clear why sulfate and sulfur analyses disagree.

5.5 Aluminum and silica

There is a minor decrease in aqueous silica concentrations along the centerline in Area A from approximately 27 ppm SiO_2 to about 20 ppm. Based on saturation indices, this slight decrease may be accounted for by the precipitation of some form of SiO_2, because Area A groundwaters are supersaturated with respect to quartz, and/or by the precipitation of allophane, an amorphous alumino-silicate (e.g. Paces, 1973, 1978) which is near saturation along most of the centerline. The relatively poor accuracy of silica analyses (Morin, 1985) precludes a more thorough discussion.

Aluminum displays a distinct trend of decreasing concentrations from the inner core to the outer zone (Fig. 10). Initially, amorphous $Al(OH)_3$ was suspected as the major aluminum precipitate, but the log SI diagram for this compound (Fig. 15) shows no area where saturation is fully attained. On the other hand, the form of $Al(OH)_3$ that would be expected to precipitate from Area A groundwaters could be more crystalline than the truly amorphous material, as sometimes found with $Fe(OH)_3$. Assuming that more crystalline $Al(OH)_3$ is represented by a log SI value of -1 on Fig. 15, $Al(OH)_3$ precipitation appears to be occurring only in a small region near the dam between M20 and M8; this region is the "$Al(OH)_3$ sub-region" discussed in the third paper of this series: Morin and Cherry (1988b). To account for the remainder of aqueous

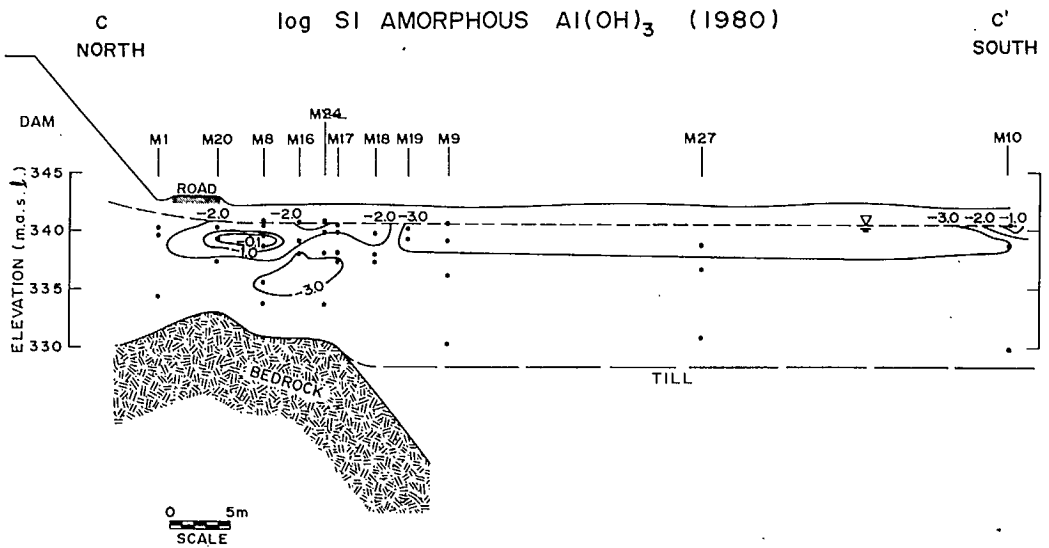

Fig. 15. Log. SI amorphous $Al(OH)_3$ for the centerplane.

aluminum depletion, there must be at least one more Al mineral forming in other regions of the centerplane.

As already mentioned, allophane is near saturation through most of the centerline; however, because only minor amounts of silica are apparently lost from solution, allophane at best can only account for a comparable, minor loss of aluminum from solution such as occurs in the outer zone. Morin (1983) attempted to identify the mineral through saturation indices and found several similar aluminum minerals that were near saturation. In order to simplify the problem, the mineral found to satisfactorily reproduce the remaining aluminum trends was boehmite (e.g. Cristoph et al., 1979; May et al., 1979), which is a dehydrated form of $Al(OH)_3$, i.e. AlOOH, and has a solubility about 2 orders-of-magnitude less than amorphous $Al(OH)_3$ when expressed as $[Al^{3+}][OH^-]^3$ in parallel with the pQ concept for ferric-oxide minerals. By using a log SI value of -2 to represent boehmite saturation on Fig. 15, boehmite can generally account for aluminum precipitation along most of the centerline.

5.6 Other major/minor ions, metals, and stable isotopes

Most other ions in Seepage Area A waters (Table 1) decrease in concentration through the neutralization zone. The possible processes accounting for the decreases are ion exchange, precipitation, and co-precipitation. Adsorption onto the sand is believed to be a minor process because of the relatively low CEC of Area A sands and the probable swamping of exchange sites by aqueous iron. Also, saturation indices indicate precipitation of other major, minor and metal solutes is not likely. Consequently, co-precipitation appears to be the regulator of many ions. For example, the incorporation or substitution of Mn into calcite-siderite and the co-precipitation of Zn and other metals with Al-OH minerals are common. A higher CEC on the actively precipitating minerals may exist, but the differentiation of this effect from other types of co-precipitation (e.g., crystal lattice substitution) is difficult and not made as part of this study.

The stable isotopes examined in this study are: ^{13}C, ^{2}H, and ^{18}O. Along the centerline of the plume from piezometer M1 to M9 (Fig. 4), $\delta^{13}C$ of DIC remains essentially constant at approximately $-19.5‰$ (relative to PDB standard), suggesting the solid-phase carbonate which undergoes replacement and eventual dissolution has a similar ^{13}C isotopic composition to the DIC and that the saturated zone in Area A is essentially a closed system (discussed in detail in Morin, 1983). The latter conclusion is also supported by the apparent lack of oxygen transport to the saturated zone for iron oxidation and the apparent retention of radon-222 gas in the saturated zone (second paper of this series: Morin et al., 1988).

For inner-core water at M1, δ^2H is $-84‰$ and $\delta^{18}O$ is $11.8‰$ (relative to SMOW), which are typical of meteoric waters in the northern Ontario region

of Canada. However, after passing through the major zone of $Al(OH)_3$ precipitation, the values change to −81‰ and -10.9‰, respectively, at M8. At M18, values are −78‰ and −11.1‰, respectively. Such variations over distances of meters to ten meters in fast flowing groundwater systems are often not expected. Nevertheless, this variation in stable isotopes is additional evidence for the unusually high geochemical reactivity of Area A groundwaters.

6. SUMMARY

The contaminant plume in Area A, which lies directly beneath the water table, can be divided into three geochemical zones based on aqueous concentrations. The *inner core* contains low-pH, high-iron, high-sulfate groundwater, which is actually unaltered seepage from the tailings. As inner-core water flows downgradient, it enters the *neutralization zone*, in which pH is neutralized and aqueous concentrations of most ions decrease significantly. As neutralization-zone water flows downgradient, it enters the pH-neutral *outer zone*, in which relatively minor geochemical reactions occur. The outer zone also includes pH-neutral mill-process water which is found at depth in the sand aquifer.

Comparisons of yearly data from 1979 to 1984 indicate the inner core and neutralization zone are migrating downgradient at a rate of about 1–2 m yr^{-1}. Because groundwater velocity is about 440 m yr^{-1}, contaminant concentration fronts are highly retarded with respect to groundwater movement.

A conceptual geochemical model is proposed that accounts for observed aqueous trends and explains the observed retardation rates. The major reactions of the model are precipitation-dissolution of the calcite-siderite solid solution, gypsum, Al-OH minerals, and Fe-OH minerals. Aqueous buffering reactions are also important, but are not amenable to simple stoichiometric calculations and, thus, are not addressed in this first paper. Stoichiometric "cell-and streamtube" calculations demonstrate how the conceptual model generally accounts for aqueous trends and migration rates. However, more precise calculations with a computer program will be discussed in the third paper of this series (Morin and Cherry, 1988b). Co-precipitation apparently causes the observed decreases in concentrations of most other major, minor, and metal solutes. Noticeable changes in the stable isotopes, ^{2}H and ^{18}O of water, occur over a distance of several meters, while ^{13}C remains essentially constant.

ACKNOWLEDGEMENTS

Many thanks for helpful discussions and assistance go to Neil Dubrovsky (USGS, Sacramento, CA), Paul Buszka (USGS, Austin, TX), Eric Reardon (University of Waterloo), and Tom Holm (Illinois State Water Survey). This study was supported by Strategic Grant G0679 from the National Science and

Engineering Research Council (Canada), by research agreements with CANMET (Energy, Mines, and Resources, Canada) and with Rio Algom Limited, and by National Uranium Tailings Program (EMR Canada) contracts to Morwijk Enterprises and the Institute for Groundwater Research.

REFERENCES

Abdul, A.S. and Gillham, R.W., 1984. Numerical simulation studies of the groundwater discharge to streams from abandoned uranium mill tailings. Final Report for Contract OST83-00283 with the National Uranium Tailings Program, Department of Energy, Mines, and Resources Canada.

Ball, J.W., Jenne, E.A. and Nordstrom, D.K., 1979. WATEQ2 – A computerized chemical model for trace and major element speciation and mineral equilibria of natural waters. In: E.A. Jenne (Editor), Chemical Modeling Of Natural Waters. Am. Chem. Soc., Symp. Ser., 93: 815–835.

Barker, J.F. and Chatten, S., 1982 A technique for determining low concentrations of total carbonate in geologic materials. Chem. Geol., 36: 317–323.

Blair, R.D., 1981. Hydrogeochemistry of an inactive pyritic uranium tailings basin, Nordic mine, Elliot Lake, Ontario. M.Sc. theisis, Department of Earth Sciences, University of Waterloo, Waterloo, Ont., 125 pp.

Blair, R.D., Cherry, J.A., Lim, T.P. and Vivyurka, A.J., 1980. Groundwater monitoring and contaminant occurrence at an abandoned tailings area, Elliot Lake, Ontario. Proc. 1st Int. Conference on Uranium Mine Waste Disposal, Vancouver. Soc. Min. Eng. Am. Inst. Min. Eng., New York, NY, pp. 411–444.

Blowes, D., 1983. The influence of the capillary fringe on the quantity and quality of streamflow generation in inactive uranium tailings impoundment. M. Sc. thesis, Department of Earth Sciences, University of Waterloo, Waterloo, Ont.

Cherry, J.A., Blackport, R.A., Dubrovsky, N.M., Gillham, R.W., Lim, T.P., Murray, D., Reardon, E.J. and Smyth, D.J.A., 1980. Subsurface hydrology and geochemical evolution of inactive pyritic tailings in the Elliot Lake uranium district, Canada. Proc. 3rd Symposium on Uranium Tailings Management, Colorado State University, Fort Collins, CO.

Cherry, J.A., Shepherd, T.A. and Morin, K.A., 1982. Chemical composition and geochemical behavior of contaminated groundwater at uranium tailings impoundments. Soc. Min. Eng. AIME, Annu. Meet. Dallas, Texas, February 14–18. Preprint No. 82–114.

Cherry, J.A., Gillham, R.W., Andersen, F.G. and Johnson, P.E., 1983. Migration of contaminants in groundwater at a landfill: A case study. Part 2, Groundwater monitoring devices. J. Hydrol., 63: 31–49.

Cherry, J.A., Morin, K.A. and Dubrovsky, N.M., 1984. Modelling of contaminant migration in acidic groundwater plumes at uranium tailings impoundments: ADNEUT3. Final report for National Uranium Tailings Program (Energy, Mines, Resources Canada) Contract OST83-00284, 105 pp.

Christoph, G.G., Corbato, C.E., Hoffman, D.A. and Tettenhorst, R.T., 1979. The crystal structure of boehmite. Clays Clay Miner., 27: 81–86.

Davé, N.K., Lim, T.P. and Vivyurka, A.J., 1981. Chemical and radioisotope distribution profiles in an abandoned uranium tailings pile. Proc. 4th Symposium on Uranium Mill Tailings Management, Fort Collins, CO., October, 1981.

Dubrovsky, N.M., 1986. Geochemical evolution of inactive pyritic tailings in the Elliot Lake Uranium District. Ph.D. thesis, Department of Earth Sciences, University of Waterloo, Waterloo, Ont.

Dubrovsky, N.M., Morin, K.A., Cherry, J.A. and Smyth, D.J.A., 1984. Uranium tailings acidification and subsurface contaminant transport in a sand aquifer. Water Pollut. Res. J. Can., 19: 55–89.

Dubrovsky, N.M., Cherry, J.A., Reardon, E.J. and Vivyurka, A.J., 1985. Geochemical evolution of inactive pyritic tailings in the Elliot Lake Uranium District. Can. Geotech. J., 22: 110–127.

Goldsmith, J.R., 1959. Some aspects of the geochemistry of carbonates. In: P.H. Abelson (Editor), Researches in Geochemistry, John Wiley and Sons, Inc., New York, NY.

Langmuir, D. and Whittemore, D.O., 1971. Variations in the stability of precipitated ferric oxyhydroxides. In: R.F. Gould (Editor), Nonequilibrium Systems in Natural Waters. Am. Chem. Soc., Adv. Chem. Ser. 106, 342 pp.

Lippmann, F., 1980. Phase diagrams depicting aqueous solubility of binary mineral systems. Neues Jahrb. Mineral., Abh. 139: 1–25.

Masch, F.D. and Denny, K.J., 1966. Grain-size distribution and its effect on the permeability of unconsolidated sands. Water Resour. Res., 2: 655–677.

May, H.M., Helmke, P.A. and Jackson, M.L., 1979. Gibbsite solubility and thermodynamic properties of hydroxy-aluminum ions in aqueous solution at 25°C. Geochim. Cosmochim. Acta, 43: 861–868.

Morin, K.A., 1983. Prediction of subsurface contaminant transport in acidic seepage from uranium tailings impoundments. Ph.D. thesis, Department of Earth Sciences, University of Waterloo, Waterloo, Ont. Volumes I and II.

Morin, K.A., 1985. 1984 Geochemical study of the acidic contaminant plume near the Nordic Main uranium-tailings impoundment, Elliot Lake, Ontario. Final Report for Contract OSQ84-00229 with the National Uranium Tailings Program (Energy, Mines, and Resources Canada).

Morin, K.A., 1986. Validity of redox measurements in hydrogeologic studies. In: G. van der Kamp and M. Madunicky. Compilers, Proc. Third Canadian Hydrogeologic Conference, International Association of Hydrogeologists, Saskatoon, Sask., April 21–23, 1986.

Morin, K.A. and Cherry, J.A., 1986. Trace amounts of siderite near a uranium-tailings impoundment, Elliot Lake, Ontario, and its implication in controlling contaminant migration in a sand aquifer. Chem. Geol., 56: 117–134.

Morin, K.A. and Cherry, J.A., 1988a. Field investigation of a small-diameter, cylindrical, contaminated groundwater plume emanating from a pyritic uranium-tailings impoundment. In: A.G. Collins and A.I. Johnson (Editors), Field Methods for Field Methods for Ground-Water Contamination Studies and their Standardization. ASTM Spec. Publ. ASTM-SP-963.

Morin, K.A. and Cherry, J.A., 1988b. Migration of acidic groundwater seepage from uranium-tailings impoundments. 3. Simulation of the conceptual model with application to Seepage Area A. J. Contam Hydrol., 2: 323–342.

Morin, K.A., Cherry, J.A., Lim, T.P. and Vivyurka, A.J., 1982. Contaminant migration in a sand aquifer near an inactive tailings impoundment, Elliot Lake, Ontario. Can. Geotech. J., 19: 49–62.

Morin, K.A., Cherry, J.A., Dave, N.K., Lim, T.P. and Vivyurka, A.J., 1988. Migration of acidic groundwater seepage from uranium-tailings impoundments. 2. Geochemical behavior of radionuclides in groundwater. J. Contam. Hydrol., 2: 305–322.

Nicholson, R.V., 1984. Pyrite oxidation in carbonate-buffered systems: experimental kinetics and control by oxygen diffusion in a porous medium. Ph.D. thesis, Department of Earth Sciences, University of Waterloo, Waterloo, Ont.

Nordstrom, D.K., Jenne, E.A. and Ball, J.A., 1979. Redox equilibria of iron in acid mine waters. In: E.A. Jenne (Editor), Chemical Modeling in Aqueous Systems. Am. Chem. Soc. Symp. Ser. 93.

Paces, T., 1973. Steady-state kinetics and equilibrium between ground water and granitic rock. Geochim. Cosmochim. Acta, 37: 2641–2663.

Paces, T., 1978. Reversible control of aqueous aluminum and silica during the irreversible evolution of natural waters. Geochim. Cosmochim. Acta, 42: 1487–1493.

Smyth, D.J.A., 1981. Hydrogeologic and geochemical studies above the water table in an inactive uranium tailings impoundment near Elliot Lake, Ontario. M.Sc. thesis, Department of Earth Sciences, University of Waterloo, Waterloo, Ont.

Sung, W. and Morgan, J.J., 1980. Kinetics and product of ferrous iron oxygenation in aqueous systems. Environ. Sci. Technol., 14: 561–568.

Whittemore, D.O. and Langmuir, D., 1975. The solubility of ferric oxyhydroxides in natural waters. Ground Water, 13: 359–365.